POLITECNICO DI TORINO
Repository ISTITUZIONALE

Electrospun nanofibers for improved angiogenesis: Promises for tissue engineering applications

Original
Electrospun nanofibers for improved angiogenesis: Promises for tissue engineering applications / Nazarnezhad, S.; Baino, F.; Kim, H. -W.; Webster, T. J.; Kargozar, S.. - In: NANOMATERIALS. - ISSN 2079-4991. - ELETTRONICO. - 10:8(2020), p. 1609. [10.3390/nano10081609]

Availability:
This version is available at: 11583/2903314 since: 2021-05-29T17:37:21Z

Publisher:
MDPI AG

Published
DOI:10.3390/nano10081609

Terms of use:

This article is made available under terms and conditions as specified in the corresponding bibliographic description in the repository

Publisher copyright

(Article begins on next page)

12 October 2024

nanomaterials

MDPI

Review

Electrospun Nanofibers for Improved Angiogenesis: Promises for Tissue Engineering Applications

Simin Nazarnezhad [1], Francesco Baino [2,*], Hae-Won Kim [3,4,5], Thomas J. Webster [6] and Saeid Kargozar [1,*]

1 Tissue Engineering Research Group (TERG), Department of Anatomy and Cell Biology, School of Medicine, Mashhad University of Medical Sciences, Mashhad 917794-8564, Iran; smn.nazarnezhad@yahoo.com
2 Institute of Materials Physics and Engineering, Applied Science and Technology Department, Politecnico di Torino, Corso Duca degli Abruzzi 24, 10129 Torino, Italy
3 Department of Biomaterials Science, School of Dentistry, Dankook University, Cheonan 31116, Korea; kimhw@dku.edu
4 Institute of Tissue Regeneration Engineering (ITREN), Dankook University, Cheonan 31116, Korea
5 Department of Nanobiomedical Science & BK21 PLUS NBM Global Research Center for Regenerative Medicine Research Center, Dankook University, Cheonan 31116, Korea
6 Department of Chemical Engineering, Northeastern University, 360 Huntington Avenue, Boston, MA 02115, USA; th.webster@neu.edu
* Correspondence: francesco.baino@polito.it (F.B.); kargozarsaeid@gmail.com (S.K.)

Received: 26 July 2020; Accepted: 14 August 2020; Published: 17 August 2020

Abstract: Angiogenesis (or the development of new blood vessels) is a key event in tissue engineering and regenerative medicine; thus, a number of biomaterials have been developed and combined with stem cells and/or bioactive molecules to produce three-dimensional (3D) pro-angiogenic constructs. Among the various biomaterials, electrospun nanofibrous scaffolds offer great opportunities for pro-angiogenic approaches in tissue repair and regeneration. Nanofibers made of natural and synthetic polymers are often used to incorporate bioactive components (e.g., bioactive glasses (BGs)) and load biomolecules (e.g., vascular endothelial growth factor (VEGF)) that exert pro-angiogenic activity. Furthermore, seeding of specific types of stem cells (e.g., endothelial progenitor cells) onto nanofibrous scaffolds is considered as a valuable alternative for inducing angiogenesis. The effectiveness of these strategies has been extensively examined both in vitro and in vivo and the outcomes have shown promise in the reconstruction of hard and soft tissues (mainly bone and skin, respectively). However, the translational of electrospun scaffolds with pro-angiogenic molecules or cells is only at its beginning, requiring more research to prove their usefulness in the repair and regeneration of other highly-vascularized vital tissues and organs. This review will cover the latest progress in designing and developing pro-angiogenic electrospun nanofibers and evaluate their usefulness in a tissue engineering and regenerative medicine setting.

Keywords: nanofibers; scaffolds; electrospinning; angiogenesis; tissue engineering; wound healing; nanotechnology

1. Introduction

Therapeutic angiogenesis has been considered as a fundamental process for developing efficient tissue-engineered constructs, which facilitates the mass transfer of oxygen, nutrients, growth factors, signaling molecules, and metabolic waste from the extracellular milieu to cells, and vice versa [1,2]. As most cells in the body are found at a distance of 100–200 μm from the nearest capillary, oxygen, nutrients, and waste products reach them via the diffusion process. Therefore, successful tissue regeneration and replacement approaches require a highly vascularized network, reaching within

100–200 μm of cells to prevent an ischemic condition and tissue necrosis [3,4]. Therefore, tissue constructs should integrate a three dimensional (3D) interconnected capillary network to facilitate the repair and regeneration of human tissues (e.g., bone and skin). The initiation and ingrowth of a vascular network into transplanted tissues are followed by pro-angiogenic signaling pathways in which pro-angiogenic growth factors (mainly vascular endothelial growth factor (VEGF) and basic fibroblast growth factor (bFGF)) are major constituents. In particular, an ordered and sequential interaction happens between pro-angiogenic growth factors and extracellular matrix (ECM) formation, leading to a synergistic effect on both the adhesion and proliferation of endothelial cells [5–9]. In addition, the surrounding cells, including pericytes and smooth muscle cells (SMCs), in the angiogenic microenvironment also participate in the maturation and stabilization of newly formed vascular networks [10–13]. Table 1 summarizes some of the bioactive molecules (e.g., growth factors, cytokines, and so on) involved in the angiogenesis process and their functions in chronological order.

Table 1. Some of the major angiogenic bioactive molecules that play critical roles in angiogenesis (sorted by time of occurrence) [14]. VEGF, vascular endothelial growth factor.

Bioactive Molecule	Function
VEGF family	Stimulating angiogenesis, permeability, and leukocyte adhesion
Angiopoetin1 (Ang1) and Tie2	Stabilizing vessels and inhibiting permeability
Platelet-derived growth factor-BB (PDGF-BB)	Recruiting of smooth muscle cells (SMCs)
Transforming growth factor-β (TGF-β1)	Stimulating extracellular matrix (ECM) production
Fibroblast growth factor (FGF) and hepatocyte growth factor (HGF)	Stimulating angio/arteriogenesis
Matrix metalloproteinase (MMPs)	Matrix remodeling, release and activation of growth factors
Plasminogen activator inhibitor-1 (PAI-1)	Stabilizing nascent vessels
Nitric oxide synthase (NOS)	Promoting angiogenesis and vasodilation

However, the use of transplanted materials carries a series of limitations (e.g., availability, risk of immune rejection [15,16]) and, therefore, attention has turned to formulate manmade implantable grafts [17]. Along with recent advancements in developing 3D scaffolds capable of promoting angiogenesis, electrospun nanofibers have gained much attention owing to their numerous advantages including its biomimetic in vivo ECM structure, high surface area to volume ratio, versatility in polymer selection (natural and synthetic types or their composites), easy process, and tunable integration with other scaffolds like hydrogels and 3D bio-printed constructs. Promoting angiogenesis by electrospun mats has been one of the most desirable therapeutic targets in which several researchers have globally tried to make angiogenic nanofibrous scaffolds and determine parameters that affect angiogenesis [18,19]. For example, it has been reported that electrospun scaffold architectures (pore size and fiber diameter) might modulate macrophage and mast cell responses, and thereby affect the secretion of VEGF [20,21]. Table 2 shows some parameters of fibrous scaffolds effective on the angiogenesis process.

Table 2. Parameters of fibrous scaffolds that may affect angiogenesis.

Parameter	Possible Effect on Angiogenesis	Ref(s)
Porosity	A minimum porosity of 30 to 40 μm is required for metabolite exchange and endothelial cell (EC) entrance	[22,23]
Pore size	Pores greater than 300 μm are required for new blood vessel formation of the constructs	[24,25]
Fiber orientation	Aligned nanofibers promote neovascularization	[26]
Heparin-functionalized nanofibers	Promoting angiogenesis through binding to angiogenic growth factors such as VEGF, HGF, and FGF-2	[27]
Polymer degradation	Slower polymer degradation leads to greater cell mobilization and angiogenesis owing to less acidic environment formation (however, electrospun nanofibrous mats are not mentioned)	[28]
Scaffold stiffness	Greater surface stiffness leads to higher EC spreading and a larger number and greater length of new sprout formation (however, nanofibers are not mentioned)	[29]

It has been previously documented that nanofibrous scaffolds made of ECM-like filaments (e.g., collagen) could serve as suitable substrates for endothelial cell adhesion, proliferation, and migration, leading to the promotion of vascularization [30–32]. Furthermore, electrospun nanofibers have been widely used as suitable drug delivery vehicles for the sustained release of various

angiogenesis-inducing growth factors, cytokines, and other bioactive molecules [33–36]. It should be noted that the co-delivery of angiogenic growth factors and other bioactive molecules by nanofibrous scaffolds is also suggested to improve tissue repair and regeneration [37].

In addition to growth factors and cytokines, electrospun nanofibers have been utilized to load and control the release of angiogenic small molecules (e.g., angiogenin) and phytochemicals (e.g., curcumin) in order to accelerate the healing process [38,39]. However, it should be highlighted that the angiogenic efficacy of such substances is strongly dose-dependent [40,41]. It is worth mentioning that surface functionalization of nanofibrous scaffolds by angiogenic bioactive molecules was also proven as a feasible approach for promoting tissue repair and regeneration [42,43]. Apart from these molecules, enhanced neovascularization could be achieved by adding inorganic elements (e.g., cerium and europium) to electrospun scaffolds [44–46]. Although there are several inorganic elements with the potential ability to induce angiogenesis, the risk of cytotoxicity and genotoxicity still limits their extensive use in tissue engineering applications [47]. In order to overcome this restriction, highly controlled doping of angiogenic elements to the structure of bioceramics (e.g., calcium phosphates and bioactive glasses) is suggested. In this sense, the incorporation of angiogenic metal-doped bioceramics into electrospun nanofibers sets up new possibilities for biomedical engineers to fabricate effective tissue substitutes [48,49].

From a biological point of view, different somatic and stem cells (e.g., endothelial cells (ECs) and mesenchymal stem cells (MSCs)) could be easily seeded onto nanofibrous scaffolds to promote angiogenesis, and subsequently accelerate the wound-healing process in injured sites [50]. This benefit originates from the inherent ability of cells to secret pro-angiogenic factors as well as to facilitate tubulogenesis (formation and expansion of the vascular lumen into newly formed branches) [51,52]. Moreover, the composition of electrospun mats may trigger and enhance the angiogenic activity of cells. For instance, nanofibrous scaffolds made of collagen-poly(ε-caprolactone) (PCL) and BG nanoparticles were used to efficiently deliver endothelial progenitor cells (EPCs) for enhancing wound healing. The incorporation of BG nanoparticles into the constructs may lead to accelerated wound healing as a result of enhanced cell viability and angiogenesis [53].

In the present review, we aim to introduce electrospun nanofibers as excellent 3D structures in angiogenesis-modulated tissue healing and highlight their potential as drug delivery systems. For this purpose, the key role of angiogenesis in tissue repair and regeneration is briefly presented, and then different scenarios applied to fabricate angiogenic electrospun nanofibrous scaffolds will be discussed. Finally, therapeutic applications of angiogenic nanofibers in both hard and soft tissues are introduced to determine their progress in tissue engineering and regenerative medicine. To the best of the authors' knowledge, this review is the first of its kind dealing with the critical role of electrospun nanofibrous scaffolds in the regulation of angiogenesis and subsequent wound healing process critical for all tissue engineering applications.

2. Angiogenesis: A Critical Procedure in Tissue Engineering

Angiogenesis is defined as the process of sprouting new capillaries from pre-existing blood vessels, which occurs in sequential steps, including the following: (1) breakdown of the vascular basement membrane; (2) the expansion and alignment of ECs, which leads to lumen formation; (3) sprouting and migration via penetrating the ECM; (4) vessel maturation; and (5) stabilization [54–56]. After any injury to the body, the rupture of blood vessels appears as the most common event and their rebuilding is of great significance in the wound healing process. Therefore, biomedical engineers and biologists have focused on the development of functional tissue-engineered constructs to quickly re-establish blood flow to damaged tissues [57–59]. Indeed, blood supply provides oxygen, essential nutrients, signaling molecules, and growth factors to the injured sites, while removing waste by-products from the surrounding environment of cells. All of these events result in the improved viability of tissue-engineered constructs to prevent ischemic and necrotic conditions [60,61].

To date, numerous strategies have been exploited to promote neovascularization, including the fabrication of vascularized tissues [62], the incorporation of pro-angiogenic molecules into 3D constructs [63], and physicochemical treatment of scaffolds [64]. In this regard, the electrospinning of nanofibers has been proposed as an easy fabrication method to prepare angiogenic 3D constructs for accelerating the wound healing process.

3. Electrospun Nanofibers: A Brief Overview

In the past few years, impressive research has been directed towards electrospun nanofibers for numerous biomedical applications such as tissue repair and tissue regeneration as well as drug delivery [65]. Electrospinning provides the possibility of fabricating a wide variety of ECM-mimicking scaffolds with a high surface area and porosity by using both natural and synthetic polymers [66,67]. The basic components of an electrospinning system consist of (1) a high-voltage power supply, (2) a syringe with a metallic needle (to transfer the polymer solution), and (3) a metallic collector (to deposit nanofibers) [68–70]. In this process, a high voltage (in the range of 10–20 kV) is applied between the polymer solution in the syringe (as a positive electrode) and the collector plate (as a negative electrode), which leads to nanofiber formation by solvent evaporation from the jet [68,71–74].

It has been well understood that processing conditions applied by the electrospinning machine could influence the characteristics of the final produced electrospun fibers (mats) (Table 3). These situations could be summarized in specific groups including the electrospinning environment (e.g., humidity and temperature); electrospinning parameters (e.g., applied voltage (in the range of kV), needle tip to collector distance (cm), and the flow rate of the solution (μL/min)); and polymer solution properties like polymer molecular weight, solution viscosity, and solvent volatility [75–79]. For example, the fiber diameter increases not only owing to the enhanced concentration and higher molecular weight of the polymers used, but also by increasing the solution flow rate. However, the increase in other parameters for the polymers used such as electrical conductivity could lead to decreased fiber diameter [75].

Table 3. The effects of electrospinning parameters on nanofibers.

Parameters	Effects on Nanofiber Properties	Ref.
Polymer parameters		
Polymer concentration	Higher polymer concentration leads to increased fiber diameter and higher pore size and porosity	[21]
Solution viscosity	Increased viscosity results in increased nanofiber uniformity and diameter and reduced beaded morphology	[80]
Molecular weight of polymer	Increased molecular weight leads to higher nanofiber diameter and less bead formation	[81]
Surface tension	Less surface tension leads to proper jet initiation	[82]
Conductivity	Higher solution conductivity leads to decreased fiber diameter	[83]
Electrospinning parameters		
Applied voltage	Initially decreases nanofiber diameter and then increases after a point	[84]
Needle tip to collector distance	Too short and too long distances lead to bead formation	[85]
Flow rate	Higher flow rate leads to bead formation, decreased flow rate leads to a decrease in fiber diameter	[86]
Temperature	Higher temperature leads to decreased fiber diameter	[87]
Humidity	Increase in humidity leads to circular pores on the fibers	[88]

According to the number and structure of the nozzles and polymers used, the electrospinning technique could be divided into two categories, including uniaxial and multiaxial electrospinning [89]. Uniaxial electrospinning is a simple and common method to fabricate a mixture of polymers and drugs, but it lacks the potential of achieving a finely-controlled drug release rate [90]. On the contrary, it is possible to produce core-shell nanofibers with enhanced drug release efficacy (the drug is loaded into the core) using coaxial electrospinning [91,92]. In the last decade, triaxial electrospinning has motivated researchers to fabricate triaxial nanofibers with a highly controlled release profile. In this context, a three-layered electrospun mat could be constructed with the same polymeric composition, but different drug content, which generates a gradient distribution of active ingredients [93]. In addition, multiaxial electrospinning allows for delivering multiple therapeutic agents with different release time profiles [94]. The structure and shapes of the produced mats could be divided into multilayer [95],

hollow [96,97], side-by-side [98], twisted [99,100], and porous surface nanofibers [101,102]. It is worth mentioning that different shapes may affect the physicochemical and functional properties of final product. Moreover, surface modification of the nanofiber mats (e.g., covalent and non-covalent immobilization and plasma treatment) is also considered as a critical parameter in determining the physico-chemical and biological properties like drug delivery efficiency [68,103,104]. On the basis of the desired applications, a broad range of raw materials could be used to fabricate electrospun mats, including natural polymers (e.g., collagen, chitosan, alginate, and hyaluronic acid), synthetic polymers (e.g., PCL, poly(lactic acid) (PLA) and poly(lactic-co-glycolic acid) (PLGA)), and their combinations [75]. It is worth noting that the development of electrospun nanofiber-reinforced composites is being currently studied to further improve the physico-chemical and biological properties of the final construct [105].

4. Electrospun Nanofibers Meet Angiogenesis

Recent evidence has revealed that enhanced angiogenesis can be achieved by applying nanofibrous mats. As depicted in Figure 1, angiogenic inducing electrospun mats could be easily fabricated by adding specific materials (e.g., bioactive glasses (BGs)) and bioactive molecules (e.g., VEGF) to polymeric substrates. In addition, seeding progenitor/stem cells (e.g., EPCs) onto fibrous scaffolds has been proposed as another reasonable approach regarding enhanced neo-vessel formation. It has been identified that inherent characteristics of fibers including pore size, porosity, and alignment are key determinants for the outcome [106]. For example, small pore size is a major obstacle for cell infiltration and vascularization. The pore size of electrospun nanofibers can be modulated by properly acting on electrospinning parameters and/or by combining electrospinning with gas foaming, salt leaching, and electrospraying [107]. According to the literature, a pore size of 300 μm in the nanofibrous scaffolds has been identified as an optimal dimension to induce new vessel formation [108].

Prior experimental studies have confirmed the intrinsic angiogenic properties of some natural and synthetic polymers (e.g., collagen [109], elastin [110], and PLA [111]) and their composites (Table 4). As an illustration, hyaluronic acid oligosaccharide-modified collagen nanofibers have been proven to promote the proliferation and endothelialization by ECs [112]. However, scientific evidence is limited in the case of angiogenic natural polymers, and experimental studies on synthetic polymers are fairly more abundant than those with naturally-derived polymers. PCL-based electrospun nanofibers are among the most used nanofibrous mats as angiogenic biomaterials in different regenerative models including choroidal neovascularization [113], artery substitute for long-term implantation [114], and smooth muscle tissue [115]. Moreover, PCL copolymers such as poly(lactide-co-ε-caprolactone) (PLCL) have been shown to induce angiogenesis after implantation in a rat model, in which more and larger vessels were formed and penetrated the construct after intraperitoneal implantation compared with subcutaneous implantation [116]. It should be pointed out that other PCL-based constructs (e.g., nanofiber-hydrogel composites) have also shown the ability to induce angiogenesis. For instance, Li et al. produced nanofibrous PCL-hyaluronic acid hydrogel composites that mimicked the structure and mechanical properties of the soft tissue ECM. This network allowed for the infiltration of macrophages and guided them to the regenerative phenotype, which ultimately led to the promoted expression of pro-angiogenic growth factors and cytokines including VEGF-D, matrix metalloproteinase-2 (MMP2), matrix metalloproteinase-3 (MMP3), and matrix metalloproteinase-19 (MMP19) after subcutaneous injection in rat and rabbit models [117]. Another synthetic polymer that was shown to have pro-angiogenic properties is poly(L-lactic acid) (PLLA) [118]. PLLA could stimulate the migration of vascular smooth muscle cells (VSMCs) via an NF-κB-dependent pathway, which in turn could promote angiogenesis [119].

Table 4. A summary of polymeric nanofibers with the ability to promote angiogenesis. PCL, poly(ε-caprolactone); PLA, poly(lactic acid).

Polymer(s)	Fiber Diameter	Biomedical Application	Remark(s)	Ref.
Expanded 3D PCL nanofiber	Not mentioned	Neovascularization after subcutaneous implantation	Promoted cell infiltration and tissue integration Enhanced regenerative response owing to increased expression of CD68, CCR7, and CD163 markers	[120]
Poly [2-bis-(3 octyloxyphenyl) quinoxaline-5,8-diyl-alt-thiophene-2,5-diyl] (TQ1)	Not mentioned	Angiogenesis	A semiconducting luminescent polymer that could be visualized in situ up to 90 days after subcutaneous implantation using fluorescence imaging Limited inflammation and formation of small capillaries around the fibers	[121]
PLA	657 +/− 101 nm for random and 568+/− 81 nm for aligned nanofibers	Angiogenesis and neurogenesis	Radially aligned nanofibers supported neuronal migration Long-term viability and integration of newly generated neurons	[111]
PHB, PCL, PLA, and PA (polyamide)	Not mentioned	Angiogenesis and cardiac repair	Among the scaffolds used, PHB had the most biocompatibility, biodegradability, angiogenic and potential, as well as expression of pro-inflammatory cytokines including interleukin (IL)-1β, IL-4, IL-6, IL-10, IL-13, and IFN-γ after epicardial implantation	[122]
PCL/collagen/PEO	250 nm +/− 73 nm	Angiogenesis	Lower sprouting vessels in the aligned scaffold, but earlier vascularization in the center of the construct compared with nonwoven scaffolds using microCT scan images	[30]
PDLLA/PCL/gelatin	500–700 nm	Angiogenesis	Anisotropically and heterogeneously aligned scaffold Excellent mechanical properties and bioactivity	[123]
PHB	1603 +/− 73 nm	Angiogenesis and skin reconstruction	Good biocompatibility Advanced properties compared with PCL for skin regeneration Polarization of macrophages to the M2 phenotype	[124]

Abbreviations: PHB: Polyhydroxybutyrate, PEO: polyethylene oxide, PDLLA: Poly(D,L-lactic acid).

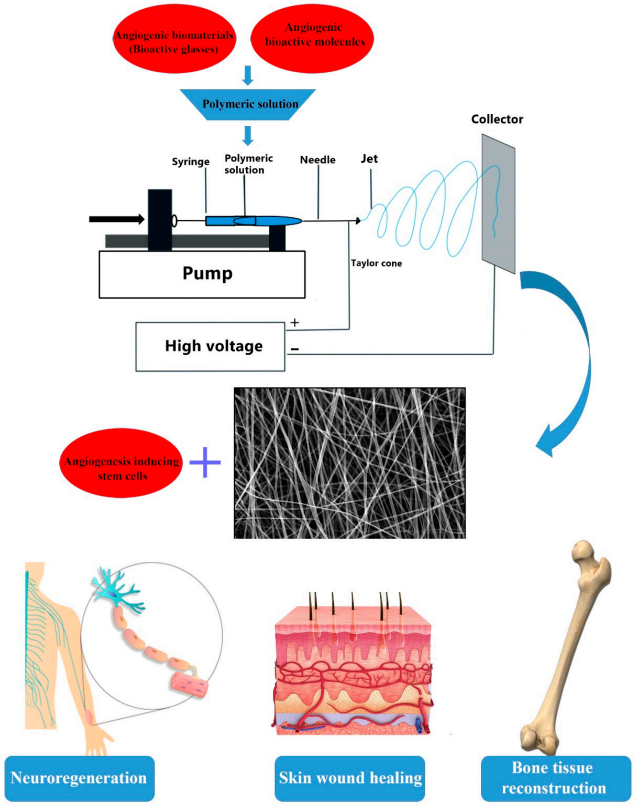

Figure 1. Neo-vessel formation can be induced by applying electrospun nanofibers containing pro-aniogenic bioactive molecules (e.g., vascular endothelial growth factor (VEGF)), angiogenesis inducing progenitor/stem cells (endothelial progenitor cells, EPCs), and angiogenic biomaterials (e.g., bioactive glasses). The fabricated angiogenic nanofibers could be applied for accelerating wound healing process for both hard (e.g., the bone) and soft tissues (e.g., the skin and the peripheral nerves).

The use of electrospun nanofibrous composites based on a combination of both natural and synthetic polymers has also been examined to promote angiogenesis. As an illustration, Gugutkov et al. fabricated composite scaffolds of electrospun fibrinogen (FBG)-PLA to take advantage of the excellent cell recognition properties of native FBG and biomechanical properties of PLA [26]. The obtained data revealed that the aligned nanofibers promoted an elongated EC shape and enhanced cell mobility, leading to faster wound coverage, while the stellate-like morphology of the ECs was observed on the random nanofibers. In addition, the results of a nitric oxide (NO) release assay showed that human umbilical vein endothelial cells (HUVECs) possessed increased functionality on random nanofibers as compared with the aligned counterparts. The authors concluded that random nanofibers might support endothelialization, whereas aligned ones could guide neovascularization of implants.

4.1. Nanofibers as Delivery Systems of Angiogenic Substances

Electrospun nanofibers benefit from a high loading efficiency of therapeutic agents owing to a large surface area to volume ratio compared with other conventional nanoscale delivery vehicles like liposomes, polymeric micelles, and complexes. Furthermore, the tunable and tailored properties of the polymer matrix (e.g., porosity, diameter, and morphology) provide the possibility of incorporating various drugs into electrospun scaffolds, thus leading to effective localized delivery of drugs to the targeted tissue [125]. Several methods have been developed to enhance the encapsulation efficiency of therapeutic agents into the nanofibrous mats, hindering their burst release, including pre-electrospinning (blending, emulsion, and coaxial electrospinning/electrospraying) as well as post-electrospinning methods (chemical immobilization, physical adsorption, and layer-by-layer assembly) [126,127]. To date, a huge number of attempts have been made to create pro- and

anti-angiogenic nanofibrous mats for potential use in a wide range of biomedical applications, from cancer therapy to tissue engineering and regenerative medicine. However, the main concern of the following section is to present and discuss the most important experimental studies concerning angiogenic nanofibrous mats in either pristine or modified forms (different types of chemicals, bioactive molecules, cells, as well as biomaterials), which can facilitate the generation of vascularized tissue-engineered constructs.

4.1.1. Pro-Angiogenic Growth Factor/Hormone-Loaded Nanofibrous Scaffolds

Encapsulation of pro-angiogenic growth factors into electrospun nanofibers is an effective and direct strategy to promote angiogenesis in different physiological and pathological conditions. To date, a large number of experimental studies have successfully encapsulated pro-angiogenic growth factors (mainly VEGF) into nanofibrous mats by means of different techniques, such as coaxial electrospinning, to achieve sustained release profiles [128–131]. For example, in order to accelerate endothelialization along the lumen of graft, composite grafts were fabricated by co-electrospinning of chitosan hydrogel/polyethylene glycol (PEG)-b-poly(L-lactide-co-ε-caprolactone) (PLCL) loaded with VEGF as the inner layer and platelet-derived growth factor (PDGF)-loaded emulsion/PLCL nanofibers as the outer layer. Four weeks after construct and engraftment into the rabbit carotid artery, vascular endothelial cells (VECs) and vascular smooth muscle cells (VSMCs) were observed on the lumen and exterior of the vascular grafts, respectively [132]. In another study, genipin-crosslinked electrospun gelatin mats and were immersed in a human VEGF-containing solution (50 ng/mg dry mat, 5 mL/mg of dry mats) to stimulate early angiogenesis in vitro and in vivo [34]. The results proved the bioactivity and pro-angiogenic capacity of VEGF, which was retained for up to 14 days.

On the basis of the literature, it can be noticed that the simultaneous incorporation of multiple pro-angiogenic growth factors into electrospun nanomats may accelerate the angiogenesis process [132,133]. The pro-angiogenic factors VEGF [134,135], bFGF [136–138], and PDGF-BB [139] proved to recapitulate the in vivo physiological conditions, leading to functional and mature blood vessel formation. For instance, VEGF triggers the growth and proliferation of endothelial cells [140]; modulates the vascular permeability [141]; and, in combination with bFGF, induces the recruitment of endothelial cells, while PDGF is responsible for new vessel stabilization [142]. For instance, Lai et al. fabricated an electrospun construct consisting of collagen/hyaluronic acid nanofibers with a programmable release (up to one month) of VEGF, PDGF (with final concentration of 0.2 μg/μL, which was adsorbed in 10 mg gelatin nanoparticles for both VEGF and PDGF), bFGF, and EGF either embedded in the nanofibers or encapsulated in the gelatin nanoparticles to accelerate the wound closure rate [133].

It should be highlighted that innovative techniques, such as the combination of electrospinning with electrospraying, have also been utilized to deliver growth factors [126]. In this context, DeVolder et al. developed VEGF-encapsulated PLGA microparticles (10 μg/mL of VEGF), which were electrosprayed simultaneously with electrospun PLA fibers. This approach resulted in a sustained release of VEGF from PLGA microparticles, leading to a larger number and size of mature blood vessels (according to the CAM assay after 1 week), while the aligned PLA fibers without VEGF-encapsulated PLGA microparticles guided the orientation of new blood vessel formation [143].

It has been well demonstrated that hormones can mediate angiogenesis either by action on endothelial cells or through regulating pro-angiogenic factors like VEGF [144]. In this sense, PCL nanofibrous mats containing the triiodothyronine (T3) hormone were fabricated and showed an increased rate of endothelial cell proliferation, migration, and angiogenesis [145]. Heparin is an anticoagulation hormone that triggers the proliferation of HUVECs [146]. In order to promote the blood compatibility of nanofibers, coaxial electrospun scaffolds were constructed in which the inner layer was comprised of PLGA/collagen nanofibers modified by mesoporous silica nanoparticles-grafted with PEG and heparin and the outer layer was composed of polyurethane nanofibers to improve mechanical properties. This composite enhanced the proliferation of both endothelial cells and smooth muscle cells by immunostaining of CD31 and alpha-smooth muscle actin (α-SMA) markers after

a rabbit carotid artery implantation, respectively [147]. In addition, heparinized nanofibrous scaffolds also showed the ability to promote the proliferation of ECs, and were thus proposed for the production of bioengineered blood vessels [148].

4.1.2. Nanofibers Incorporating Phytochemicals and Other Bioactive Molecules

Phytochemicals form a major part of organic materials applied in tissue engineering and regenerative medicine [40,149–152]. Experimental data showed the pro-angiogenic capacity of some specific types of phytochemicals; for example, icariin is able to induce angiogenesis through activating the MEK/ERK- and PI3K/Akt/eNOS-dependent signal pathways in human endothelial cells [153]. However, it should be highlighted that some of the phytochemicals (e.g., curcumin) showed pro- or anti-angiogenic activities in a dose-dependent manner [154–156]. To date, a series of studies have shown the usability of phytochemical-incorporated electrospun nanofibers regarding pro-angiogenic strategies [43,157]. On the basis of the literature, there is still a scientific gap in this area and researchers are suggested to pay more focus to phytochemical-incorporated electrospun nanofibers for inducing angiogenesis.

Other bioactive molecules can also trigger angiogenesis including metallic ions, platelet-rich plasma (PRP) [158,159], ECM derivatives, recombinant proteins [160–163], and decellularized matrices [164]. Plenty of experimental studies have been conducted to survey the feasibility of such approaches to promote angiogenesis. For example, the effectiveness of copper impregnation into polymeric matrices (9 wt% and 4 wt% of $CuSO_4$ in dimethylformamide with a polyurethane/copper volume ratio of 8:1 and 8:0.5 (*v*/*v*%) in two separate studies, respectively) when making the composite electrospun scaffolds clearly proved pro-angiogenic strategies [165,166]. In the case of natural components, increased secretion of VEGF and bFGF proteins was observed by applying a 3D bi-layer scaffold of a decellularized human amniotic membrane and electrospun nanofibrous silk fibroin seeded with adipose tissue-derived MSCs [167].

4.2. Bioactive Glass- and Bioceramic-Incorporated Electrospun Scaffolds

There is sufficient scientific evidence on the pro-angiogenic capacity of glasses, glass-ceramics, and calcium phosphates (CaPs) [168–173]. The main reason is attributed to the release of pro-angiogenic ions (e.g., Si^{4+}) from BGs and glass-ceramics to the surrounding environment [174]. It should be emphasized that the incorporation of metallic elements (e.g., Cu^{2+} and Co^{2+}) into BGs and glass-ceramics is a common approach to enhance their angiogenic potential [175,176]. Previously, the fabrication of electrospun nanofibers from strontium- and copper-doped BGs has been reported as a promising approach in regards to improving neovascularization [177]. In addition, the usability of 3D composite nanofibrous scaffolds made of glasses and polymeric matrices has been examined for pro-angiogenic strategies [178–181]. Differentiation of human endometrial stem cells (EnSCs) into endothelial-like cells was previously reported using gelatin/chitosan/bioactive glass (GEL/CS/BG) nanofibrous scaffolds [182]. In the presence of FGF-2 and VEGF, EnSCs differentiated into ECs and then were cultured onto the glass-containing scaffolds. The nanofibrous scaffolds were prepared by adding 0.5, 1.5, and 3% wt of BG nanoparticles (BGNPs) to a GEL/CS solution; the diameter of the obtained nanofibers increased along with reducing the BG content in the GEL/CS scaffolds. The cellular experiments showed that the nanofibrous scaffolds with 1.5% BGNPs were more suitable substrates for EC differentiation and possible use for blood vessel regeneration applications. In another study, PLA nanofibers containing calcium phosphate ormoglass particles showed the ability to promote angiogenesis via up-regulation of pro-angiogenic factors VEGF, insulin-like growth factor-2 (IGF-2), Fas ligand, granulocyte-macrophage colony-stimulating factor (GM-CSF), interleukin-1β (IL-1β), IL-6, and IL-12p70 in mammalian cells [183]. Apart from the mentioned studies, the experimental research on BG-incorporated electrospun nanofibrous scaffolds is indeed limited, and more investigations should be performed to reveal the pros and cons of BG-containing polymeric nanofibers for angiogenic promoting strategies.

CaPs were previously reviewed and introduced as materials having the potential to influence angiogenesis [169]. Therefore, the incorporation of CaPs into polymeric electrospun nanofibers is currently under investigation in the context of angiogenesis. As the biological behaviors of CaPs could be easily modified by adding trace metal ions to their structure, several studies have tried to enhance the angiogenic potential of CaPs by replacing therapeutic pro-angiogenic ions [184–187]. Ye et al. could enhance osteogenesis and angiogenesis by the incorporation of 20 wt% bioactive strontium-doped CaP nanoparticles into PCL/chitosan electrospun nanocomposite membranes via a one-step electrospinning method [188]. They reported that the nanocomposite membranes possessed similar structural properties of the native ECM and were able to support the adhesion, proliferation, and angiogenic differentiation of rat bone marrow mesenchymal stem cells (BM-MSCs) via enhancing VEGF secretion levels. Similar to the BG-incorporated electrospun nanofibrous scaffolds, more research is needed to determine which formulations may result in the best output and how much CaPs should be added to the nanofibrous scaffolds.

4.3. Cell-Laden Nanofibers for Pro-Angiogenesis Strategies

Culturing of stem cells onto nanofibrous scaffolds might result in enhanced angiogenesis; in general, various types of stem cells have been used to promote the angiogenic capacity of nanofibrous electrospun mats [189–191]. Endothelial progenitor cells, endothelial cells, mural cells like pericytes and smooth muscle cells, mesenchymal stem cells, and hematopoietic stem cells are among the most promising candidates for promoting angiogenesis as they are able to secrete pro-angiogenic growth factors and cytokines [192–195]. Regarding the outcome of numerous experimental studies, it can be stated that extracellular vesicles and exosomes containing pro-angiogenic growth factors are responsible elements for improving neovascularization [196–199]. For instance, extracellular vesicles released from human adipose-derived stem cells have been shown to promote angiogenesis through the let-7/AGO1/VEGF signaling pathway in an ischemic model of mice [198]. Despite this potent pro-angiogenic capacity, there is limited evidence of experiments in which pro-angiogenic exosomes and vesicles incorporated into the nanofibrous mats were shown to induce neovascularization. However, the encapsulation of various stem cells and EPCs secreting pro-angiogenic vesicles in electrospun nanofibers has been regarded as an efficient strategy to accelerate neovascularization in various tissues [200–202]. In this sense, EPCs were able to induce tubular structure formation into a highly porous 3D electrospun scaffold composed of PCL. The large pore size (pore size > 400 μm) of this scaffold regulated EPC behavior, that is, cell infiltration, proliferation, colonization, and new blood vessel formation [106]. Previously, the co-culturing of EPCs with perivascular cells like MSCs or fibroblasts has been proposed as a good strategy to make long-lasting and functional vascular networks [203]. In this sense, Hong et al. fabricated six-layered PCL nanofibrous constructs (12.5% w/v) and seeded both sides of each layer with endothelial cells and pericyte cells (Figure 2). The results obtained from confocal microscopy showed an embossed vascular pattern (208.8 ± 44.5 μm in height) up to 3 days post-cell culture. New blood vessel formation and maturation were also confirmed by the upregulation of VEGF and Ang-1 genes in the 6x embossed group [204]. Furthermore, co-culturing of ECs with bone and adipose tissue derived mesenchymal stem cells (BM-MSCs and AD-MSCs) led to promoted endothelial tubulogenesis [205].

Some studies also revealed the applicability of BM-MSCs- and AD-MSCs-loaded nanofibrous scaffolds in promoting angiogenesis [206–209]. With the rise of novel cell technologies, such as the methods to manipulate induced-pluripotent stem cells (iPSCs), researchers are currently able to generate iPSC-derived endothelial cells (iPSC-ECs) as a promising source of ECs for therapeutic angiogenesis [210–212]. However, there are a few reports in the literature concerning the in vivo engraftment of iPSC-ECs for boosting neovascularization. Tan et al. showed that the incorporation of iPSC-ECs into electrospun PCL/gelatin scaffolds could increase the pro-angiogenic function via enhanced expression of VEGF and placental growth factor (PLGF) [213]. Despite recent advancements of iPSCs in the field of regenerative medicine, a lack of investigation still remains a pressing issue for the use of this cell type in angiogenesis-stimulant nanofibrous mats.

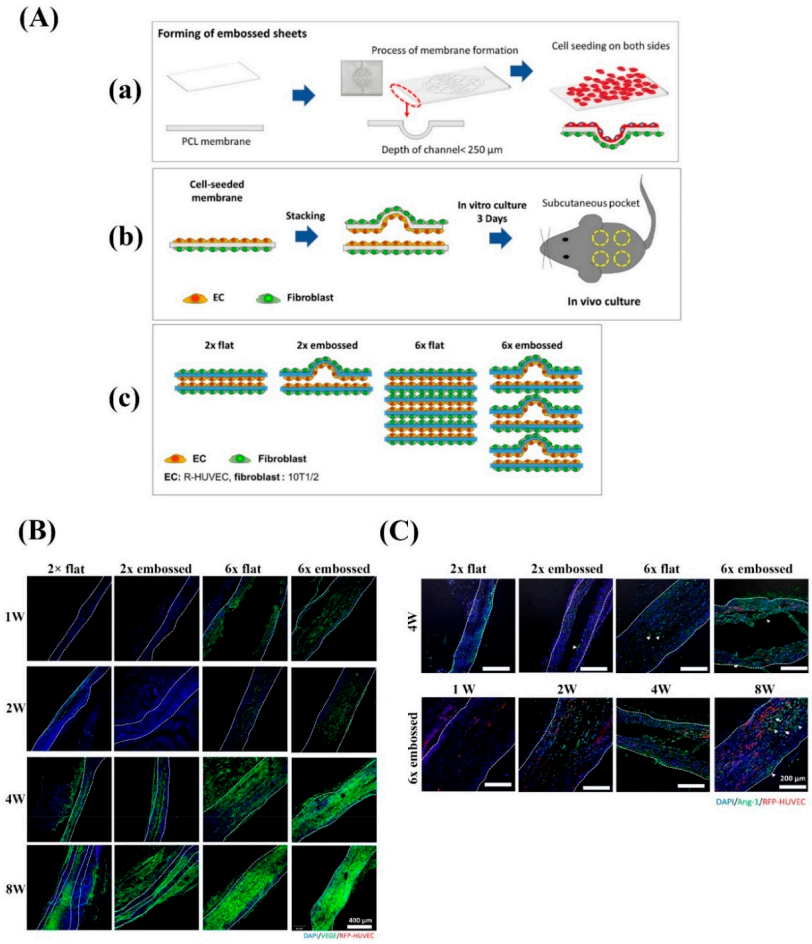

Figure 2. (**A**) A schematic representation of the preparation of electrospun nanofibrous membranes with embossed patterns for guided vascularization: (**a**) the formation of embossed sheet and plating of human ECs and mouse fibroblast cells, (**b**) stacking and incubating of the cell-laden sheets for 3 days before the implantation into subcutaneous pockets in mice, and (**c**) four different experimental groups evaluated in vivo. (**B**) Immunofluorescence images exhibiting differences in VEGF expression in different groups after 1, 2, 4, and 8 weeks of surgery; dashed lines show the edge of transplanted embossed sheets. Green: VEGF, red: human umbilical vein endothelial cell (HUVEC), blue: DAPI. (**C**) Immunofluorescence images exhibiting differences in angiopoietin 1 (Ang-1) expression in cross-sections of different groups after 1, 2, 4, and 8 weeks of surgery; dashed lines show the edge of transplanted embossed sheets. Green: Ang-1, red: HUVEC, blue: DAPI (adapted from Hong et al. [204]). PCL, poly(ε-caprolactone); EC, endothelial cell.

Table 5 summarizes a list of experiments in which various cells/nanofibrous scaffolds were applied to improve angiogenesis. As electrical stimulation can promote the angiogenesis in different tissues and cell types (including the artery [214], skeletal muscle [215], peripheral nerve [216], wound healing [217,218], endothelial cells [219,220], human mesenchymal stromal cells [221], adipose tissue-derived stem cells [222], cardiomyocytes [223], and osteoblasts [224]), it may be useful to use electrospun conducting polymer nanofibers to obtain better in vitro and in vivo results in future investigations. However, there is some evidence of using conductive polymers in hydrogel constructs with pro-angiogenic potential (such as N-carboxyethyl chitosan and oxidized hyaluronic acid-graft-aniline tetramer [225], gelatin-grafted-dopamine and polydopamine-coated carbon nanotubes [226], and polypyrrole [227]), but there is a lack of research on such polymers incorporated in electrospun nanofibers with a pro-angiogenic approach.

Table 5. Some examples of experimental studies in which pro-angiogenic factors were integrated into nanofibrous scaffolds. MSC, mesenchymal stem cell; PLGA, poly(lactic-co-glycolic acid); PEG, polyethylene glycol.

Polymer	Pro-Angiogenic Factor	Method of Integration	Remarks	Ref(s)
Cells				
PLA/PCL	hUC-MSCs	Seeding cells on the scaffold	PCL significantly increased the angiogenic potential of hUC-MSCs with no additional factors Increased migratory and pro-angiogenic potential	[228]
Polydioxan-one (PDO)	Bone marrow-derived macrophages	Seeding cells on the scaffold	Higher concentrations of polymer led to a larger fiber diameter, pore size, and porosity Increased secretion of pro-angiogenic cytokines including VEGF, bFGF, and TGF-β for the scaffolds with larger pore sizes Pore size of the scaffold is more critical than fiber diameter in macrophage polarization	[21]
PCL/gelatin	Adipose tissue-derived mesenchymal stem cells (ADSCs)	Seeding and coculturing of ADSCs and HUVECs on the scaffolds	Greater sprouting of endothelial cells, formation of a mature blood vessel-like network, and enhanced expression of tight junction proteins	[191]
PCL/gelatin/fi-bronectin	Cardiac progenitor cells (CPC)	Seeding cells on the patches	Electrospun scaffolds maintained durable CPC viability Reduced fibrotic gene expression in rat cardiac fibroblasts Tube formation of HUVECs by media collected from the nanofibrous patches demonstrating the pro-angiogenic potential of the patch	[229]
PLCL/colla-gen nanoyarn fibers	Pig iliac endothelial cells (PIECs) and MC3T3-E1 pre-osteoblastic cells	Seeding cells on nanoyarn scaffold	Formation of complex capillary-like structures after 7 days More cell infiltration into this morphology of electrospun scaffolds compared with conventional nanofibrous electrospun mats	[230]
Growth factors				
Gelatin	bFGF	Physical immobilization	Proliferation rate of HUVECs was proportional to the loading concentration of bFGF (0–100 ng/mL) The gradient growth factor distribution effects on vessel direction	[33]
Pullulan/dex-tran nanofibers loaded with fucoidan	VEGF	Physical immobilization	Increased fucoidan content led to increased retention of VEGF bioactivity and angiogenic response up to 14 days Promoted cellular infiltration and complete biodegradation of the construct up to 7 days after subcutaneous implantation in mice	[133]
Poly(estera-mide) PEA	FGF2, FGF9	Emulsion electrospinning	Sustained release and preserved bioactivity of FGF2 and FGF9 over 28 days Enhanced tubular formation	[35,231,232]
PLGA	Collagen containing VEGF	Surface coating	Improved pre-vascularization of the construct after seeding HUVECs Anastomose formation between the implanted construct and mice vasculature confirmed by immunostaining of CD31 and von Willebrand factor	[233]
Others				
PEG	bFGF and VEGF-encoding plasmids	Coaxial electrospinning	Improved cell viability and attachment and extracellular secretion of collagen IV and laminin Alleviated inflammation reaction and enhanced microvessel generation	[234]
Nylon	Insulin		Outer porous layer supports cellular infiltration and vascularization Inner low porosity layer supports cellular isolation Localized cell transplantation	[235]
PCL	Heparin and VEGF	Immersing in heparin and VEGF solution, respectively	Stimulated neovascularization with minimum immunological rejection	[236]
PLCL	Substance P		Sustained release of substance P up to 30 days Improved host cell infiltration, blood vessel formation, and MSC recruitment in vivo Existence of laminin-positive blood vessels and von Willebrand factor cells	[237]
PCL	Vitamin D3	Blending	Promoted cellular infiltration and neovascularization Reduced inflammation and infection	[238]
Silk fibroin/gelatin	Astragaloside IV		Accelerated wound healing and prevented scar formation by stimulating wound closure and increasing angiogenesis in partial-thickness burn wounds	[239]
PCL	Collagenase	Surface immobilization	Collagenase (0.01 mg/mL) promoted smooth muscle cell (SMC) migration Enhanced capillary formation after subcutaneous implantation	[240]
Gelatin/PLGA	Cobalt and PEGylated curcumin	Core-shell electrospinning	Promoted EC patterning and enhanced VEGF production	[241]
PLLA/chitosan nanofibers coated with polydopa-mine	Icariin and deferoxamine	Surface modification	Synergistic effects on osteogenesis and angiogenesis	[43]

5. Angiogenic Nanofibrous Scaffolds in Tissue Engineering

The fabrication and use of pro-angiogenic electrospun mats are of great interest in tissue engineering approaches regarding their ability to accelerate the wound healing process. Therefore, several studies have tried to implement angiogenic nanofiber mats for the reconstruction of both hard and soft tissues. In the following sections, we summarize and discuss the angiogenic electrospun nanofibrous scaffolds in the frame of tissue engineering and regenerative medicine. The reviewed studies are also collected in Table 6.

5.1. Angiogenic Nanofibers for Hard Tissue Engineering

The fundamental role of therapeutic angiogenesis has been well established during the repair and regeneration of hard tissues like bones. Local delivery of osteogenic and angiogenic growth factors (mainly bone morphogenic protein-2 (BMP2), FGF, and VEGF) via electrospun nanofibrous membranes were considered as a promising strategy for overall enhanced osteogenesis [242], in which, specifically, BMP2 enhances osteogenic differentiation of MSCs [243], VEGF promotes angiogenesis of MSCs [244], and bFGF promotes cell proliferation and migration as well as tube formation of HUVECs [245]. It is worth noting that the sequential release of various growth factors from the electrospun nanofibers could accelerate vascularized bone formation. Accordingly, Cheng et al. fabricated multilayer core-shell silk fibroin (SF)/PCL/PVA nanofibrous scaffolds containing BMP2 (10 μg/mL) and connective tissue growth factor (CTGF) (10 μg/mL) [246]. For this aim, they incorporated BMP2 into the core of the mats by applying coaxial electrospinning and then immobilized CTGF onto their surface via a layer-by-layer (LBL) self-assembly technique (Figure 3). The efficacy of the prepared scaffolds was examined in vitro and in vivo to reveal their potential in bone tissue engineering applications, with a special focus on the promotion of osteogenesis and angiogenesis. The in vitro results revealed a sustained and linear release profile for BMP2 (during 30 days) and a burst release for CTGF (during 40 days). The results of the implantation of the nanofibrous mats into a critical-size cranial defect of mice models revealed a significantly higher newly-formed bone percentage (43%) in the animals treated with the BMP2/CTGF-loaded (SF/PCL) 1:5/PVA-LBL_{20} scaffolds in comparison with the (SF/PCL) 1:5/PVA nanofibrous mats loaded with BMP2 alone after 4 weeks. The same trend was observed in the samples harvested at 8 weeks post-implantation in mice as the largest bone area and bone volume belonged to the BMP2/CTGF-loaded (SF/PCL) 1:5/PVA-LBL_{20} nanofibrous mats. Furthermore, angiogenic markers of VEGF and CD-31 were over-expressed in the animals treated with the BMP2/CTGF-loaded (SF/PCL) 1:5/PVA-LBL_{20} group. The authors concluded that sequential and dual-delivery of BMP2 and CTGF might be useful in inducing osteogenesis and angiogenesis, ultimately yielding accelerated bone formation with new blood vessels.

There are limited reports in the literature dealing with the application of bioceramic-containing polymeric nanofibrous mats for promoting angiogenesis and subsequently accelerating bone tissue healing. In this content, Oliveira et al. developed injectable composite scaffolds made of Ca-/P rich ormoglass particles prepared by a partial hydrolyzed alkoxides sol-gel method with a composition of 44.5:44.5:6:5 of $CaO:P_2O_5:Na_2O:TiO_2$ molar ratios dispersed in (hydroxypropyl) methyl cellulose (HPMC) gels (40% *w*/*v*) coated with PLA fibers [247]. They evaluated the osteogenic and angiogenic capacities of the constructs in femoral condyles of Wistar rats. The release of Ca^{2+} ions from the scaffolds had a positive impact on bone formation and angiogenesis after 3 and 6 weeks of implantation.

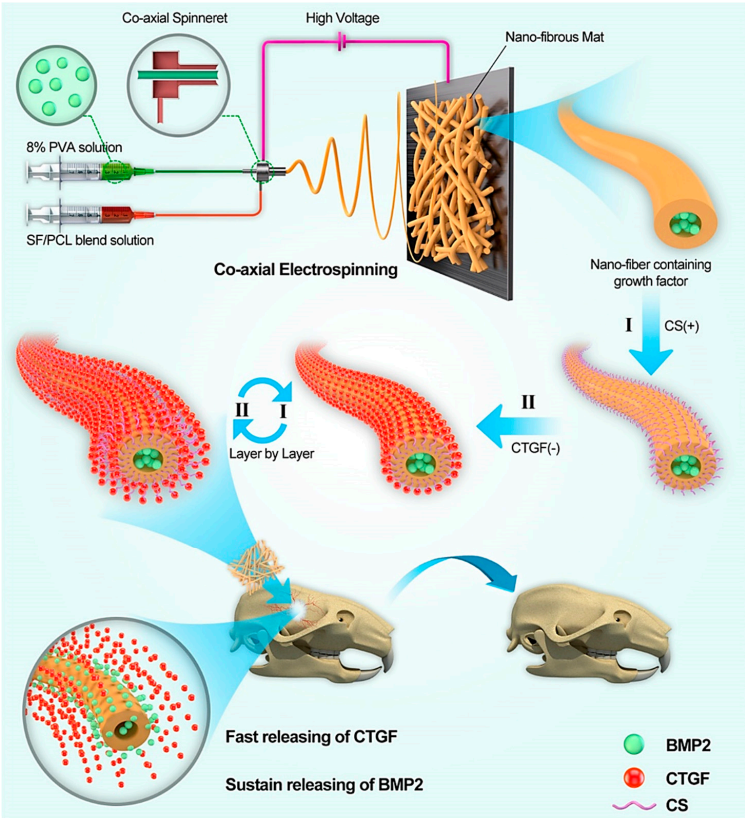

Figure 3. Schematic illustration of the bone healing process via controlled co-delivery of connective tissue growth factor (CTGF) and bone morphogenic protein-2 (BMP2) by combining the technique of coaxial electrospinning and layer-by-layer (LBL) process. BMP2 and CTGF were incorporated and attached to the core and the surface of the nanofibers, respectively (adapted from Cheng et al. [246]). SF: silk fibroin and CS: chitosan.

As the incorporation of cytokines and bioactive molecules (e.g., BMP2) into electrospun mats may have adverse effects on their bioactivity, researchers have proposed the physical adsorption method as a gold standard to retain bioactivity [248]. In this regard, 3D hybrid nanofiber aerogels were fabricated with a formulation of PLGA-collagen-gelatin (PCG) and Sr/Cu co-doped BGs fibers incorporated with E7 domain-specific BMP-2 peptides [249]. Sr^{2+} and Cu^{2+} ions were added to the glass to promote neo-bone formation and vascularization, respectively. The degradable hybrid aerogels were implanted into critical-sized defects (8 mm in diameter) created in rat calvaria to determine its efficacy in the bone healing process. Data obtained from radiography and histopathological assessments revealed a 60–70% closure of critical-sized defects in the injured sites (Figure 4).

A critical issue in bone tissue engineering is osteoclast-mediated bone resorption and osteoblast-mediated bone formation in the process of bone remodeling [250]. In 2019, Wang et al. developed mesoporous silicate nanoparticle (MSN)-based electrospun PCL/gelatin nanofibers for the dual delivery of alendronate (ALN) and silicate ions [251]. The concept behind this study was to achieve a synergetic effect in modulating bone remodeling because ALN could inhibit the bone-resorbing process through inhibiting of guanosine triphosphate-related protein expression, while silicate ions promote the bone-forming process by promoting angiogenesis and bone calcification. The release of both ALN and silicon (in the form silicate ions) from the scaffolds was observed, indicating the success of dual drug delivery using the scaffolds. The results of in vivo implantation of the ALN@MSN-loaded nanofibers in a rat critical-sized cranial defect model revealed an accelerated bone healing time (from 4 weeks to 12 weeks post-implantation), which was three times faster in comparison with the bare scaffolds.

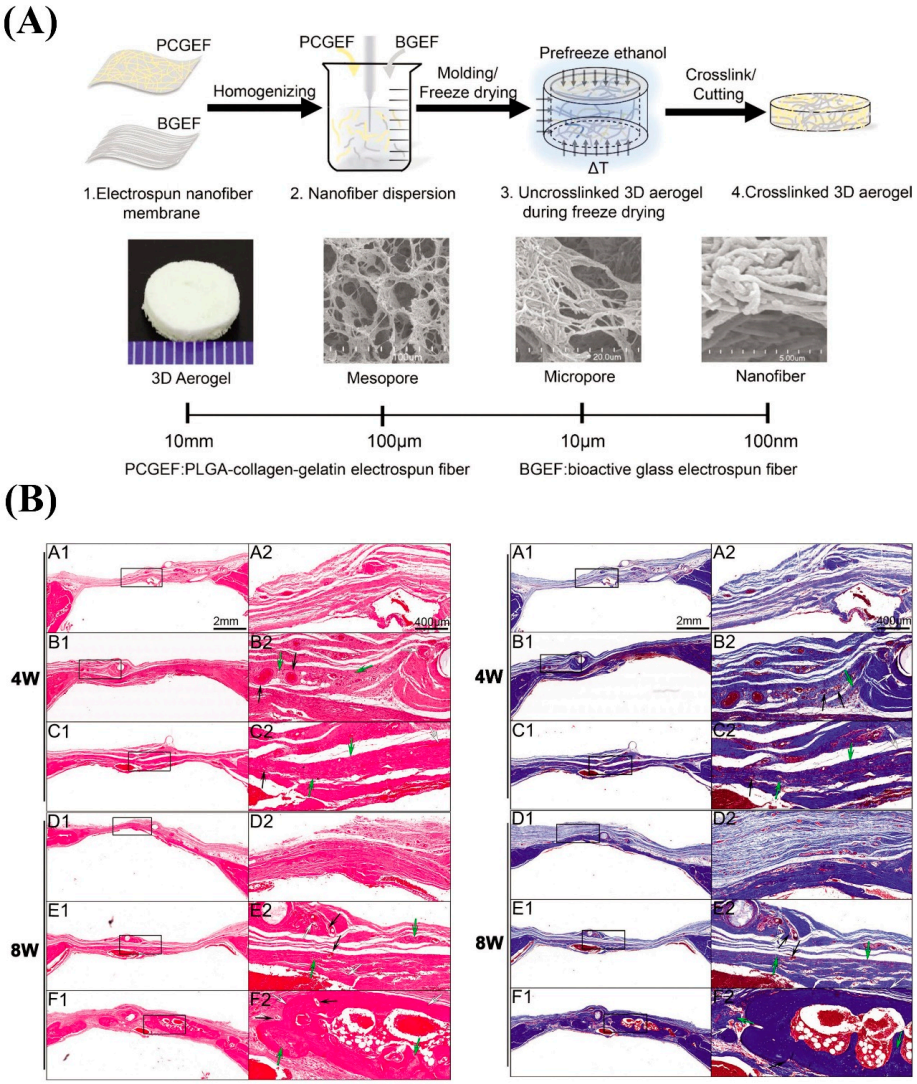

Figure 4. (**A**) Schematic representation of different steps of the preparation of the 3D hybrid nanofiber aerogels and its structure. (**B**) Images of hematoxylin and eosin-stained (left) and Masson's trichrome-stained (right) tissue slides at 4 and 8 weeks post-implantation into critical-sized calvarial defects in rats. (A1/A2, D1/D2) Unfiled defects; (B1/B2, E1/E2) the defects implanted by 3D hybrid nanofiber aerogels (PCG/BG = 60:40); and (C1/C2, F1/F2) the defects implanted by E7-BMP-2 peptide-loaded 3D hybrid nanofiber aerogel (PCG/BG = 60:40) (black arrow: blood vessel in aerogel; white arrow: aerogel residue; green arrow: new bone) (adapted from Weng et al. [249], with permission from John Wiley and Sons).

5.2. Angiogenic Nanofibers for Soft Tissue Regeneration

5.2.1. Angiogenic Nanofibrous Mats for Skin Regeneration

Angiogenesis plays a pivotal role in soft tissue wound healing, especially in the case of chronic wounds [252,253]. Several electrospun membranes have shown great abilities to improve the healing process of epidermal and dermal layers [163,254]. By highlighting the role of angiogenesis in the skin regeneration process, a multifunctional and biomimetic nanofibrous membrane was composed of fish collagen type I (COL) and bioactive glasses (BGs) using the electrospinning method [255]. The prepared nanofibers (ratio of COL/BG was 10:1) had a fiber diameter of 494 ± 193 nm and could not only promote the adhesion and proliferation of HaCaT cells, but also upregulate the expression of TGF-β and MMP-9 genes. In addition, dermal regeneration and angiogenesis were also promoted by COL/BG

nanofibrous mat regarding the increased adhesion and proliferation of human dermal fibroblasts (HDFs) ($p < 0.05$) as well as secretion of collagen type I protein and VEGF ($p < 0.05$). The histological results obtained from the cutaneous implantation of COL/BG nanofibers into rats revealed a higher formation of collagen fibers and rapid re-epithelialization and angiogenesis in the injured sites.

Diabetic wounds usually suffer from an impaired wound healing process owing to the vascular impairment resulting from the delayed secretion of pro-angiogenic factors as well as reduced proliferation and migration of ECs and tissue re-epithelialization [255–258]. In this regard, many researchers have made significant attempts to develop an efficient pro-angiogenic wound dressing for accelerating diabetic wound healing and tackling this important societal and clinical challenge [133,259]. In 2018, Ren et al. reported the successful fabrication of electrospun fibrous membranes made of poly(L-lactic acid) (PLLA) containing dimethyloxalylglycine (DMOG)-loaded mesoporous silica nanoparticles (DS) for potential usage in diabetic wound healing [260]. This system could act as a sustained release vehicle for DMOG and silicon ions, leading to stimulating the proliferation, migration, and angiogenesis-related gene expression of HUVECs in comparison with the PLLA membranes. The in vivo implantation of the constructs in the dorsal skin of diabetic mice showed an improvement in neo-vascularization, re-epithelialization, and collagen formation 15 days post-surgery.

Electrospun nanofibers have been previously used for the encapsulation and sustained release of pro-angiogenic growth factors to accelerate skin wound repair [261]. Conventional efforts have relied on the LBL assembly and coaxial electrospinning to achieve the controlled release of multiple growth factors in which the diffusion between layers is a major hindrance [262–264]. In this regard, the use of nanoparticles is suggested to obtain a more effective sustained-release [261]. It has been previously reported that neovascularization within the wound site might be improved by applying a nanofibrous scaffold composed of collagen, PCL, and bioactive glass nanoparticles (CPB) seeded with EPCs [53]. The mechanism proposed for this improvement was attributed to the activation of the HIF-1α/VEGF/SDF-1α signaling pathway in the injured site, which can result in promoted cell proliferation, granulation tissue formation, and collagen synthesis and deposition.

As an outstanding study, a research team under the supervision of Prof. Wu reported simultaneous tumor therapy and skin wound regeneration by applying electrospun micro-patterned nanocomposites incorporated with Cu_2S nanoflowers [265]. Indeed, this strategy seems to be really suitable for effectively killing of the remaining tumor cells after surgical excision of skin tumors. The authors took benefits from the photothermal capacity of Cu_2S nanoflowers and the angiogenic potential of Cu^{2+} ions in a substrate of poly(D, L-lactic acid)/PCL. The composite membranes (Cu_2S incorporated PDLLA/PCL (CS-PLA/PCL) membranes) were produced using the patterning-co-electrospinning method, which could improve the adhesion, proliferation, and angiogenesis of ECs in vitro as well as accelerate in vivo wound healing. In addition, the hyperthermia induced by laser-irradiated 30CS-PCL membranes allowed for the ablation of skin tumor cells (B16F10 cells and A375 cells) in vitro and inhibited B16F10 tumor growth in vivo.

5.2.2. Angiogenic Fibers for Neuroregeneration

It has been suggested that neural defects longer than 5 mm are difficult to recover and regenerate by themselves [266]. With regard to several limitations of autologous and allogenic transplantation of peripheral nerves [267], aligned electrospun nanofibers integrated with growth factors and/or neural stem cells and Schwann cells have been stated to be promising replacements for neurite outgrowth and peripheral nerve regeneration [268–272]. Some studies have focused on neural regeneration triggered by angiogenic electrospun nanofibers [111]. Indeed, the orientation and growth of axons can be guided by aligned nanofibrous matrices in order to allow for the formation of a vascularized network [273]. Zhang et al. investigated the neural regeneration capacity of coaxial electrospun silk fibers loaded with VEGF and brain-derived neurotrophic factor (BDNF) on cavernous nerve regeneration [274]. Two types of core-shell nanofibrous scaffolds were produced and designated

as IVOB (inner layer—2.84×10^{-1} ng/mg of VEGF/outer layer—5.80×10^{-1} ng/mg of BDNF) and IBOV (inner layer—2.84×10^{-1} ng/mg of BDNF/outer layer—5.80×10^{-1} ng/mg of VEGF). The release profile of BDNF and VEGF from the scaffolds clarified an initial burst at the first 4 days, which was followed by a stable release up to 16 days. To evaluate neovascularization and nerve regeneration capacities, the authors implanted the regenerated silk fibroin (RSF)-neat scaffolds with a length of 9 mm and a width of 2 mm into Sprague–Dawley rats. The histopathological results confirmed more nerve regeneration based on promoted angiogenesis in the inner-BDNF and outer-VEGF scaffolds compared with the inner-EGF and outer-BDNF, owing to faster release of VEGF following 8 weeks post-implantation (Figure 5).

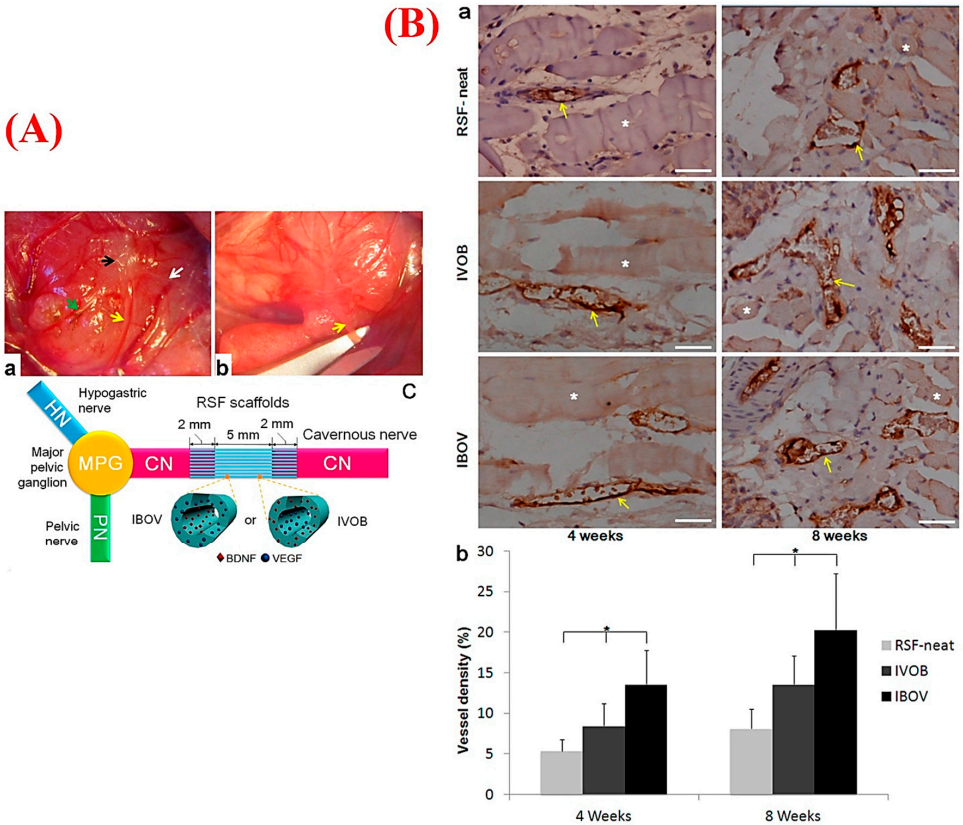

Figure 5. (**A**) Macroscopic views representing the implantation of regenerated silk fibroin (RSF) scaffolds into a rat animal model: (a) exposed major pelvic ganglion (MPG), pelvic nerve (PN), hypogastric nerve (HN), and cavernous nerve (CN) are marked as black, green, white, and yellow arrows, respectively; (b) creating the CN gap (arrow) (length of 5 mm) by scissors; and (c) schematic illustration of suturing process of RSF scaffolds and two CN ends. (**B**) Immunohistochemistry (IHC) staining of the harvested samples for evaluating new vessels in the retrieved scaffolds of RSF-neat, inner-VEGF/outer-brain-derived neurotrophic factor (BDNF) (IVOB), and inner-BDNF/outer-VEGF (IBOV) after 4 and 8 weeks of implantation (a), in which the asterisk (*) shows the scaffold fragments and the yellow arrows show vessels (bar: 100 μm); and (b) graph showing the vessel densities in (a) in which the asterisk (*) shows significant differences among the groups at each time point ($p < 0.05$). Adapted from Zhang et al. [274], with permission from American Chemical Society.

In order to regenerate a vascularized nerve tissue, Xia et al. utilized the dual delivery of NGF and VEGF within the core (via emulsion electrospinning) and sheath (by physical adsorption) of electrospun PLLA nanofibers, in which VEGF had a burst release in the first few days, while NGF could be constantly released for 30 days [275]. In vivo data confirmed the nerve regeneration process followed by neovascularization as modulated by the fibrous scaffolds after 3 months.

Table 6. A summary of experimental studies performed for improving tissue regeneration via applying angiogenic electrospun nanofibrous scaffolds. BDNF, brain-derived neurotrophic factor.

Polymer	Fiber Diameter	Therapeutic Element	Target Tissue	Remarks	Ref.
PLCL	1.16 ± 0.18 μm	Human fibroblast-derived ECM	Skin	Higher proliferation and vascular morphogenesis of HUVECs seeded on the scaffold A promising role on wound healing by increased wound closure rate, mature blood vessel density, and regenerated epidermis and skin appendages after 4 weeks post-implantation	[276]
PLGA		Angiogenin and curcumin	Skin	Maintained bioactivity and sustained release of curcumin and angiogenin in 6 days and 20 days, respectively	[38]
PCL	100 ± 20 nm	Si and Zn ions and CiH	Skin	Releasing Si ions promoted angiogenesis and skin regeneration after 14 days post-implantation Zn ions and ciprofloxacin hydrochloride (CiH) resulted in enhanced hair follicle regeneration and antibacterial activity	[277]
PCL	According to the incubation time with acetone, 2.4 ± 0.7, 1.1 ± 0.3, 0.5 ± 0.1 μm for 10 min, 1 h, and 6 h, respectively	Vasoactive intestinal peptide	Skin	Enhanced cell adhesion and proliferation Promoted wound healing by increased granulation tissue formation and angiogenesis, but not significant re-epithelialization	[278]
Gelatin and PLGA		PEGylated curcumin cobalt nanoparticles	Skin	Enhanced endothelial cell proliferation and VEGF production	[241]
PCL	218.24 ± 35.21 nm	Placental-derived bioactive molecules	Skin	Promoted adhesion, infiltration, and proliferation of fibroblasts and keratinocytes and enhanced vascularization	[163]
Cellulose acetate/gelatin	316 ± 115 nm	Nanohydroxyapa-tite (nHA)	Skin	25 mg nHA loaded in cellulose acetate/gelatin (CA/Gel) showed the highest collagen synthesis, re-epithelialization, neovascularization, and the greatest wound closure value (93.5 ± 1.6%) compared with 12.5 and 50 mg nHA	[279]
PVA and chitosan	716.5 ± 76.1 nm	Desferrioxamine	Diabetic wound	Upregulated expression of HIF-1α, VEGF, and SDF-1α Promoted interaction of fibroblasts and endothelial cells	[18]
Collagen, hyaluronic acid, and gelatin nanoparticles	486 ±151 nm and 534 ±128 nm for HA and COL nanofibers, respectively	VEGF, PDGF, bFGF, and EGF	Diabetic wound	Sustained release of growth factors up to one month owing to encapsulation of the gelatin nanoparticlesThe scaffold possesses similar mechanical properties to native skin	[133]
Heparin mimetic peptide			Diabetic wound	Accelerated wound closure and granulation tissue formation Greater expression of alpha-smooth muscle actin (α-SMA) and VEGF	[259]
Chitosan	50–200 nm		Skin	Greater cell adhesion and cell proliferation, faster regeneration of dermis and epidermis components, and well-vascularization compared with chitosan films and sponges	[254]
Polydioxanone (PDS)	1–17 μm at the concentration of 125 mg/mL PDS	Alginate beads encapsulated with NGF and chondroitinase ABC	Nerve tissue	More cellular infiltration owing to aligned nanofibers using air-gap electrospinning Vascular network formation after 3 weeks post-implantation Regenerating axons following spinal cord injury owing to trophic support and directional guidance of a scaffold	[273]
Poly-L/DL lactic acid (PLA70/30)	657 ± 101 nm for random and 568 ± 81 nm for aligned nanofibers		Damaged brain	Radially aligned nanofibers supported neuronal migration Long-term viability and integration of the newly generated neurons	[111]
Silk fibroin	1.8 ± 0.5 μm	BDNF, VEGF	Nerve tissue	De novo innervation and neovascularization indicated by a positive endothelial marker (von Willebrand factor) and innervation marker (S-100 protein) without inflammation Promoted nerve regeneration and angiogenesis after 8 weeks post-implantation	[272]
PCL/gelatin	400–700 nm	bFGF	Bone	A more controlled release of heparin-mediated bFGF up to 24 h Increased proliferation and migration of hMSCs and tubulogenesis of HUVECs Heparinized nanofibers incorporated with 50 or 100 ng/mL bFGF showed a two- and threefold increase in new bone formation, respectively	[245]
PLA	830.3 ± 211.9 nm and 853.7 ± 238.6 nm for the uncoated and coated fibers, respectively	Surface coating of polydopamine	Bone	Greater ALP activity and osteocalcin of hADSC cultured on the scaffold Up-regulation of ang-1 and vWF proteins	[171]

Table 6. *Cont.*

Polymer	Fiber Diameter	Therapeutic Element	Target Tissue	Remarks	Ref.
PCL	580 ± 80 nm	Ceramic nanoparticles including Si^{4+}, Ca^{2+}, and PO_4^{3-}	Bone	Enhanced bioactivity of PCL nanofibers owing to greater apatite formation Reduced contact angle of PCL-Ca-Si (63° ± 3°) compared with only the PCL scaffold (120° ± 10°)	[48]
PLGA	588.9 ± 110.3 nm	Heparin-mediated immobilization of VEGF Co-culture of HUVECs with human/rat MSCs	Bone	Sustained release of VEGF in conjugation with heparin Enhanced angiogenesis, which was detected by CD31 immunostaining after 3 weeks	[244]
PCL		In situ silica gelation	Bone	Enhanced water wettability and sustained release of silicon ions (28 ppm silicon ions in 14 days) Promoted tubulogenesis of HUVECs Up-regulation of pro-angiogenic markers including CD31, VEGF-A, PDGF-B, and eNOS and osteogenic markers such as COL1 A1, RUNX2, OSTX, and BMP2	[280]
Methylmethacrylate (MMA), hexylmethacrylate (HMA), and (trimethoxysilylprolyl) methacrylate (siMA)	Below 500 nm	Mg implant-coated with electrospun nanofiber containing NO	Bone	Stable and local delivery of NO for targeted tubulogenesis of HUVECs	[281]
PLLA/chitosan	Not mentioned	Icariin, deferoxamine, and polydopamine	Bone	Promoted cell adhesion, proliferation, osteogenic differentiation, and mineralization of MC3T3-E1 through upregulation of Runx-2, ALP, COL 1, and osteocalcin Up-regulation of angiogenic markers of HUVECs including eNOS, HIF-1α, VEGF, and CD31	[43]

6. Concluding Remarks and Future Perspectives

The scientific literature shows that some strategies can be potentially used to promote or somehow achieve angiogenesis in tissue substitutes, including different combinations of micro- and nano-biomaterials, stem cells, and bioactive molecules. However, angiogenesis still remains a critical issue in the development of functional engineered tissues and deserves to be investigated more in the future. In this regard, the use of electrospun nanofibrous scaffolds was evaluated as an innovative and highly versatile approach in promoting angiogenesis and subsequent accelerated tissue repair and regeneration. However, conventional electrospun nanofibers have limited potential for cell infiltration and migration, which is considered as a barrier in angiogenesis-promoted wound healing. In order to address this limitation, different strategies have been investigated to increase the pore size of electrospun mats, including melt-electrospinning. In addition, the combination of the electrospinning technique with other methods and technologies (e.g., electrospraying or bioprinting) may be useful to achieve potent angiogenic constructs.

In general, some "geometrical" and physical characteristics of the fibrous mats or scaffolds (e.g., fiber diameter, the wall thickness in the case of hollow fibers, fiber length) can be designed, controlled and finely tailored by acting on the major processing parameters of electrospinning; however, a clear picture is currently lacking on the impact that each of these features may have on angiogenesis. The spatial configuration of fibers in the mats, or in other words, the way in which the fibers are interwoven, can also play a role in many cell activities and responses, like angiogenesis. Furthermore, the composition of basic fibers and the whole construct should be taken into account; although polymers apparently play no significant role in angiogenesis if used alone, polymeric nanofibrous mats can be made pro-angiogenic by embedding bioactive molecules (e.g., growth factors like VEGF) or nano-sized inclusions (e.g., BG nanoparticles releasing metallic cations like Cu^{2+}). There is also recent evidence that incorporation of special nanoparticles (e.g., magnetic nanoparticles) in electrospun polymeric nanofibrous constructs can allow one to obtain multifunctional implants with multiple extra-functionalities, including not only angiogenesis, but also the capability of stimulating odontogenesis, thereby disclosing new horizons in the field of periodontal regeneration [282]. The main challenge for the future is perhaps a methodological one, that is, the development of a rational library associating the physico-chemical features of electrospun nanofibrous scaffolds to the following: (i) the processing parameters needed to obtain them (clear and objective reproducibility) and (ii) the biological cues that can be related to their presence/effect, with a special focus on angiogenesis.

Author Contributions: Conceptualization, S.K.; Literature search, S.N. and S.K.; writing—original draft preparation, S.N. and S.K.; writing—review and editing, F.B., H.-W.K., and T.J.W.; resources, F.B. and H.-W.K. All authors have read and agreed to the published version of the manuscript.

Funding: The authors acknowledge the partial grant support from the National Research Foundation, Republic of Korea (2018K1A4A3A01064257, 2018R1A2B3003446).

Conflicts of Interest: The authors declare no conflict of interest regarding the publication of this study.

References

1. Nomi, M.; Atala, A.; De Coppi, P.; Soker, S. Principals of neovascularization for tissue engineering. *Mol. Asp. Med.* **2002**, *23*, 463–483. [CrossRef]
2. Sarker, M.; Naghieh, S.; McInnes, A.D.; Schreyer, D.J.; Chen, X. Strategic design and fabrication of nerve guidance conduits for peripheral nerve regeneration. *Biotechnol. J.* **2018**, *13*, 1700635. [CrossRef]
3. Frerich, B.; Lindemann, N.; Kurtz-Hoffmann, J.; Oertel, K. In vitro model of a vascular stroma for the engineering of vascularized tissues. *Int. J. Oral Maxillofac. Surg.* **2001**, *30*, 414–420. [CrossRef]
4. Lovett, M.; Lee, K.; Edwards, A.; Kaplan, D.L. Vascularization strategies for tissue engineering. *Tissue Eng. Part B Rev.* **2009**, *15*, 353–370. [CrossRef]
5. Arroyo, A.G.; Iruela-Arispe, M.L. Extracellular matrix, inflammation, and the angiogenic response. *Cardiovasc. Res.* **2010**, *86*, 226–235. [CrossRef] [PubMed]

6. Schultz, G.S.; Wysocki, A. Interactions between extracellular matrix and growth factors in wound healing. *Wound Repair Regen.* **2009**, *17*, 153–162. [CrossRef]
7. Mahabeleshwar, G.H.; Feng, W.; Reddy, K.; Plow, E.F.; Byzova, T.V. Mechanisms of integrin–vascular endothelial growth factor receptor cross-activation in angiogenesis. *Circ. Res.* **2007**, *101*, 570–580. [CrossRef]
8. Somanath, P.R.; Ciocea, A.; Byzova, T.V. Integrin and growth factor receptor alliance in angiogenesis. *Cell Biochem. Biophys.* **2009**, *53*, 53–64. [CrossRef]
9. Kim, S.-H.; Turnbull, J.; Guimond, S. Extracellular matrix and cell signalling: The dynamic cooperation of integrin, proteoglycan and growth factor receptor. *J. Endocrinol.* **2011**, *209*, 139–151. [CrossRef]
10. Herbert, S.P.; Stainier, D.Y. Molecular control of endothelial cell behaviour during blood vessel morphogenesis. *Nat. Rev. Mol. Cell Biol.* **2011**, *12*, 551–564. [CrossRef]
11. Armulik, A.; Abramsson, A.; Betsholtz, C. Endothelial/pericyte interactions. *Circ. Res.* **2005**, *97*, 512–523. [CrossRef] [PubMed]
12. Gaengel, K.; Genové, G.; Armulik, A.; Betsholtz, C. Endothelial-mural cell signaling in vascular development and angiogenesis. *Arterioscler. Thromb. Vasc. Biol.* **2009**, *29*, 630–638. [CrossRef] [PubMed]
13. Ribatti, D.; Nico, B.; Crivellato, E. The role of pericytes in angiogenesis. *Int. J. Dev. Biol.* **2011**, *55*, 261–268. [CrossRef] [PubMed]
14. Carmeliet, P.; Jain, R.K. Angiogenesis in cancer and other diseases. *Nature* **2000**, *407*, 249–257. [CrossRef]
15. Dimitriou, R.; Mataliotakis, G.I.; Angoules, A.G.; Kanakaris, N.K.; Giannoudis, P.V. Complications following autologous bone graft harvesting from the iliac crest and using the RIA: A systematic review. *Injury* **2011**, *42*, S3–S15. [CrossRef]
16. Wang, W.; Yeung, K.W. Bone grafts and biomaterials substitutes for bone defect repair: A review. *Bioact. Mater.* **2017**, *2*, 224–247. [CrossRef]
17. Kargozar, S.; Ramakrishna, S.; Mozafari, M. Chemistry of biomaterials: Future prospects. *Curr. Opin. Biomed. Eng.* **2019**, *10*, 181–190. [CrossRef]
18. Chen, H.; Jia, P.; Kang, H.; Zhang, H.; Liu, Y.; Yang, P.; Yan, Y.; Zuo, G.; Guo, L.; Jiang, M. Upregulating Hif-1α by hydrogel nanofibrous scaffolds for rapidly recruiting angiogenesis relative cells in diabetic wound. *Adv. Healthc. Mater.* **2016**, *5*, 907–918. [CrossRef]
19. Gao, W.; Jin, W.; Li, Y.; Wan, L.; Wang, C.; Lin, C.; Chen, X.; Lei, B.; Mao, C. A highly bioactive bone extracellular matrix-biomimetic nanofibrous system with rapid angiogenesis promotes diabetic wound healing. *J. Mater. Chem. B* **2017**, *5*, 7285–7296. [CrossRef]
20. Abebayehu, D.; Spence, A.J.; McClure, M.J.; Haque, T.T.; Rivera, K.O.; Ryan, J.J. Polymer scaffold architecture is a key determinant in mast cell inflammatory and angiogenic responses. *J. Biomed. Mater. Res. Part A* **2019**, *107*, 884–892. [CrossRef]
21. Garg, K.; Pullen, N.A.; Oskeritzian, C.A.; Ryan, J.J.; Bowlin, G.L. Macrophage functional polarization (M1/M2) in response to varying fiber and pore dimensions of electrospun scaffolds. *Biomaterials* **2013**, *34*, 4439–4451. [CrossRef] [PubMed]
22. Madden, L.R.; Mortisen, D.J.; Sussman, E.M.; Dupras, S.K.; Fugate, J.A.; Cuy, J.L.; Hauch, K.D.; Laflamme, M.A.; Murry, C.E.; Ratner, B.D. Proangiogenic scaffolds as functional templates for cardiac tissue engineering. *Proc. Natl. Acad. Sci. USA* **2010**, *107*, 15211–15216. [CrossRef] [PubMed]
23. Oliviero, O.; Ventre, M.; Netti, P. Functional porous hydrogels to study angiogenesis under the effect of controlled release of vascular endothelial growth factor. *Acta Biomater.* **2012**, *8*, 3294–3301. [CrossRef] [PubMed]
24. Kuboki, Y.; Jin, Q.; Takita, H. Geometry of carriers controlling phenotypic expression in BMP-induced osteogenesis and chondrogenesis. *J. Bone Joint Surg.* **2001**, *83*, S105–S115. [CrossRef] [PubMed]
25. Murphy, C.M.; O'Brien, F.J. Understanding the effect of mean pore size on cell activity in collagen-glycosaminoglycan scaffolds. *Cell Adhes. Migr.* **2010**, *4*, 377–381. [CrossRef] [PubMed]
26. Gugutkov, D.; Gustavsson, J.; Cantini, M.; Salmeron-Sánchez, M.; Altankov, G. Electrospun fibrinogen–PLA nanofibres for vascular tissue engineering. *J. Tissue Eng. Regen. Med.* **2017**, *11*, 2774–2784. [CrossRef]
27. Mammadov, R.; Mammadov, B.; Guler, M.O.; Tekinay, A.B. Growth factor binding on heparin mimetic peptide nanofibers. *Biomacromolecules* **2012**, *13*, 3311–3319. [CrossRef]
28. Sung, H.-J.; Meredith, C.; Johnson, C.; Galis, Z.S. The effect of scaffold degradation rate on three-dimensional cell growth and angiogenesis. *Biomaterials* **2004**, *25*, 5735–5742. [CrossRef]

29. Mason, B.N.; Starchenko, A.; Williams, R.M.; Bonassar, L.J.; Reinhart-King, C.A. Tuning three-dimensional collagen matrix stiffness independently of collagen concentration modulates endothelial cell behavior. *Acta Biomater.* **2013**, *9*, 4635–4644. [CrossRef]
30. Klumpp, D.; Rudisile, M.; Kühnle, R.I.; Hess, A.; Bitto, F.F.; Arkudas, A.; Bleiziffer, O.; Boos, A.M.; Kneser, U.; Horch, R.E. Three-dimensional vascularization of electrospun PCL/collagen-blend nanofibrous scaffolds in vivo. *J. Biomed. Mater. Res. Part A* **2012**, *100*, 2302–2311. [CrossRef]
31. Kobayashi, H.; Terada, D.; Yokoyama, Y.; Moon, D.W.; Yasuda, Y.; Koyama, H.; Takato, T. Vascular-inducing poly (glycolic acid)-collagen nanocomposite-fiber scaffold. *J. Biomed. Nanotechnol.* **2013**, *9*, 1318–1326. [CrossRef] [PubMed]
32. Kenar, H.; Ozdogan, C.Y.; Dumlu, C.; Doger, E.; Kose, G.T.; Hasirci, V. Microfibrous scaffolds from poly (l-lactide-co-ε-caprolactone) blended with xeno-free collagen/hyaluronic acid for improvement of vascularization in tissue engineering applications. *Mater. Sci. Eng. C* **2019**, *97*, 31–44. [CrossRef]
33. Montero, R.B.; Vial, X.; Nguyen, D.T.; Farhand, S.; Reardon, M.; Pham, S.M.; Tsechpenakis, G.; Andreopoulos, F.M. bFGF-containing electrospun gelatin scaffolds with controlled nano-architectural features for directed angiogenesis. *Acta Biomater.* **2012**, *8*, 1778–1791. [CrossRef]
34. Del Gaudio, C.; Baiguera, S.; Boieri, M.; Mazzanti, B.; Ribatti, D.; Bianco, A.; Macchiarini, P. Induction of angiogenesis using VEGF releasing genipin-crosslinked electrospun gelatin mats. *Biomaterials* **2013**, *34*, 7754–7765. [CrossRef] [PubMed]
35. Said, S.S.; Yin, H.; Elfarnawany, M.; Nong, Z.; O'Neil, C.; Leong, H.; Lacefield, J.C.; Mequanint, K.; Pickering, J.G. Fortifying Angiogenesis in Ischemic Muscle with FGF9-Loaded Electrospun Poly (Ester Amide) Fibers. *Adv. Healthc. Mater.* **2019**, *8*, 1801294. [CrossRef]
36. Mulholland, E.J.; Ali, A.; Robson, T.; Dunne, N.J.; McCarthy, H.O. Delivery of RALA/siFKBPL nanoparticles via electrospun bilayer nanofibres: An innovative angiogenic therapy for wound repair. *J. Control. Release* **2019**, *316*, 53–65. [CrossRef]
37. Rather, H.A.; Patel, R.; Yadav, U.C.; Vasita, R. Dual drug-delivering polycaprolactone-collagen scaffold to induce early osteogenic differentiation and coupled angiogenesis. *Biomed. Mater.* **2020**, *15*, 045008. [CrossRef]
38. Mo, Y.; Guo, R.; Zhang, Y.; Xue, W.; Cheng, B.; Zhang, Y. Controlled dual delivery of angiogenin and curcumin by electrospun nanofibers for skin regeneration. *Tissue Eng. Part A* **2017**, *23*, 597–608. [CrossRef]
39. Zhu, Z.; Liu, Y.; Xue, Y.; Cheng, X.; Zhao, W.; Wang, J.; He, R.; Wan, Q.; Pei, X. Tazarotene released from aligned electrospun membrane facilitates cutaneous wound healing by promoting angiogenesis. *ACS Appl. Mater. Interfaces* **2019**, *11*, 36141–36153. [CrossRef] [PubMed]
40. Kargozar, S.; Baino, F.; Hoseini, S.J.; Verdi, J.; Asadpour, S.; Mozafari, M. Curcumin: Footprints on cardiac tissue engineering. *Expert Opin. Biol. Ther.* **2019**, *19*, 1199–1205. [CrossRef]
41. Selvaprithviraj, V.; Sankar, D.; Sivashanmugam, A.; Srinivasan, S.; Jayakumar, R. Pro-angiogenic molecules for therapeutic angiogenesis. *Curr. Med. Chem.* **2017**, *24*, 3413–3432. [CrossRef] [PubMed]
42. Rujitanaroj, P.-O.; Aid-Launais, R.; Chew, S.Y.; Le Visage, C. Polysaccharide electrospun fibers with sulfated poly (fucose) promote endothelial cell migration and VEGF-mediated angiogenesis. *Biomater. Sci.* **2014**, *2*, 843–852. [CrossRef] [PubMed]
43. Liu, H.; Wen, W.; Chen, S.; Zhou, C.; Luo, B. Preparation of Icariin and Deferoxamine functionalized poly (l-lactide)/chitosan micro/Nanofibrous membranes with synergistic enhanced Osteogenesis and angiogenesis. *ACS Appl. Bio Mater.* **2018**, *1*, 389–402. [CrossRef]
44. Park, I.-S.; Mahapatra, C.; Park, J.S.; Dashnyam, K.; Kim, J.-W.; Ahn, J.C.; Chung, P.-S.; Yoon, D.S.; Mandakhbayar, N.; Singh, R.K.; et al. Revascularization and limb salvage following critical limb ischemia by nanoceria-induced Ref-1/APE1-dependent angiogenesis. *Biomaterials* **2020**, *242*, 119919. [CrossRef]
45. Augustine, R.; Nethi, S.K.; Kalarikkal, N.; Thomas, S.; Patra, C.R. Electrospun polycaprolactone (PCL) scaffolds embedded with europium hydroxide nanorods (EHNs) with enhanced vascularization and cell proliferation for tissue engineering applications. *J. Mater. Chem. B* **2017**, *5*, 4660–4672. [CrossRef]
46. Kargozar, S.; Baino, F.; Hoseini, S.J.; Hamzehlou, S.; Darroudi, M.; Verdi, J.; Hasanzadeh, L.; Kim, H.-W.; Mozafari, M. Biomedical applications of nanoceria: New roles for an old player. *Nanomedicine* **2018**, *13*, 3051–3069. [CrossRef]
47. Kargozar, S.; Baino, F.; Hamzehlou, S.; Hamblin, M.R.; Mozafari, M. Nanotechnology for angiogenesis: Opportunities and challenges. *Chem. Soc. Rev.* **2020**, *49*, 5008–5057. [CrossRef]

48. Meka, S.R.K.; Agarwal, V.; Chatterjee, K. In situ preparation of multicomponent polymer composite nanofibrous scaffolds with enhanced osteogenic and angiogenic activities. *Mater. Sci. Eng. C* **2019**, *94*, 565–579. [CrossRef]
49. Rahmani, A.; Hashemi-Najafabadi, S.; Eslaminejad, M.B.; Bagheri, F.; Sayahpour, F.A. The effect of modified electrospun PCL-nHA-nZnO scaffolds on osteogenesis and angiogenesis. *J. Biomed. Mater. Res. Part A* **2019**, *107*, 2040–2052. [CrossRef]
50. Fu, Y.; Guan, J.; Guo, S.; Guo, F.; Niu, X.; Liu, Q.; Zhang, C.; Nie, H.; Wang, Y. Human urine-derived stem cells in combination with polycaprolactone/gelatin nanofibrous membranes enhance wound healing by promoting angiogenesis. *J. Transl. Med.* **2014**, *12*, 274. [CrossRef]
51. Xu, K.; Cleaver, O. Tubulogenesis during blood vessel formation. *Semin. Cell Dev. Biol.* **2011**, *229*, 993–1004. [CrossRef]
52. Dragoni, S.; Laforenza, U.; Bonetti, E.; Lodola, F.; Bottino, C.; Berra-Romani, R.; Carlo Bongio, G.; Cinelli, M.P.; Guerra, G.; Pedrazzoli, P. Vascular endothelial growth factor stimulates endothelial colony forming cells proliferation and tubulogenesis by inducing oscillations in intracellular Ca^{2+} concentration. *Stem Cells* **2011**, *29*, 1898–1907. [CrossRef] [PubMed]
53. Wang, C.; Wang, Q.; Gao, W.; Zhang, Z.; Lou, Y.; Jin, H.; Chen, X.; Lei, B.; Xu, H.; Mao, C. Highly efficient local delivery of endothelial progenitor cells significantly potentiates angiogenesis and full-thickness wound healing. *Acta Biomater.* **2018**, *69*, 156–169. [CrossRef] [PubMed]
54. Katoh, M. Therapeutics targeting angiogenesis: Genetics and epigenetics, extracellular miRNAs and signaling networks. *Int. J. Mol. Med.* **2013**, *32*, 763–767. [CrossRef] [PubMed]
55. Potente, M.; Gerhardt, H.; Carmeliet, P. Basic and therapeutic aspects of angiogenesis. *Cell* **2011**, *146*, 873–887. [CrossRef] [PubMed]
56. Carmeliet, P. Angiogenesis in life, disease and medicine. *Nature* **2005**, *438*, 932–936. [CrossRef]
57. Rouwkema, J.; Khademhosseini, A. Vascularization and angiogenesis in tissue engineering: Beyond creating static networks. *Trends Biotechnol.* **2016**, *34*, 733–745. [CrossRef] [PubMed]
58. Foresti, R.; Rossi, S.; Pinelli, S.; Alinovi, R.; Barozzi, M.; Sciancalepore, C.; Galetti, M.; Caffarra, C.; Lagonegro, P.; Scavia, G. Highly-defined bioprinting of long-term vascularized scaffolds with Bio-Trap: Complex geometry functionalization and process parameters with computer aided tissue engineering. *Materialia* **2020**, *9*, 100560. [CrossRef]
59. Richards, D.; Jia, J.; Yost, M.; Markwald, R.; Mei, Y. 3D bioprinting for vascularized tissue fabrication. *Ann. Biomed. Eng.* **2017**, *45*, 132–147. [CrossRef]
60. Blinder, Y.; Mooney, D.; Levenberg, S. Engineering approaches for inducing blood vessel formation. *Curr. Opin. Chem. Eng.* **2014**, *3*, 56–61. [CrossRef]
61. Novosel, E.C.; Kleinhans, C.; Kluger, P.J. Vascularization is the key challenge in tissue engineering. *Adv. Drug Deliv. Rev.* **2011**, *63*, 300–311. [CrossRef] [PubMed]
62. Cui, H.; Zhu, W.; Nowicki, M.; Zhou, X.; Khademhosseini, A.; Zhang, L.G. Hierarchical fabrication of engineered vascularized bone biphasic constructs via dual 3D bioprinting: Integrating regional bioactive factors into architectural design. *Adv. Healthc. Mater.* **2016**, *5*, 2174–2181. [CrossRef] [PubMed]
63. Wu, L.; Gu, Y.; Liu, L.; Tang, J.; Mao, J.; Xi, K.; Jiang, Z.; Zhou, Y.; Xu, Y.; Deng, L. Hierarchical micro/nanofibrous membranes of sustained releasing VEGF for periosteal regeneration. *Biomaterials* **2020**, *227*, 119555. [CrossRef]
64. Haerst, M.; Ahrens, M.; Seitz, V.; Wintermantel, E. Electrospinning of commercially available medical silicone rubber. *Biomed. Technol.* **2014**, *s1*, 59.
65. Stocco, T.D.; Bassous, N.J.; Zhao, S.; Granato, A.E.; Webster, T.J.; Lobo, A.O. Nanofibrous scaffolds for biomedical applications. *Nanoscale* **2018**, *10*, 12228–12255. [CrossRef]
66. Abrigo, M.; McArthur, S.L.; Kingshott, P. Electrospun nanofibers as dressings for chronic wound care: Advances, challenges, and future prospects. *Macromol. Biosci.* **2014**, *14*, 772–792. [CrossRef]
67. Rim, N.G.; Shin, C.S.; Shin, H. Current approaches to electrospun nanofibers for tissue engineering. *Biomed. Mater.* **2013**, *8*, 014102. [CrossRef]
68. Wang, J.; Windbergs, M. Functional electrospun fibers for the treatment of human skin wounds. *Eur. J. Pharm. Biopharm.* **2017**, *119*, 283–299. [CrossRef]
69. Yadav, R.; Balasubramanian, K. Metallization of electrospun PAN nanofibers via electroless gold plating. *RSC Adv.* **2015**, *5*, 24990–24996. [CrossRef]

70. Magisetty, R.; Kumar, P.; Gore, P.M.; Ganivada, M.; Shukla, A.; Kandasubramanian, B.; Shunmugam, R. Electronic properties of Poly (1, 6-heptadiynes) electrospun fibrous non-woven mat. *Mater. Chem. Phys.* **2019**, *223*, 343–352. [CrossRef]
71. Tahalyani, J.; Datar, S.; Balasubramanian, K. Investigation of dielectric properties of free standing electrospun nonwoven mat. *J. Appl. Polym. Sci.* **2018**, *135*, 46121. [CrossRef]
72. Agarwal, S.; Wendorff, J.H.; Greiner, A. Progress in the field of electrospinning for tissue engineering applications. *Adv. Mater.* **2009**, *21*, 3343–3351. [CrossRef]
73. Simon, S.; Balasubramanian, K. Facile immobilization of camphor soot on electrospun hydrophobic membrane for oil-water separation. *Mater. Focus* **2018**, *7*, 295–303. [CrossRef]
74. Simon, S.; Malik, A.; Kandasubramanian, B. Hierarchical electrospun super-hydrophobic nanocomposites of fluoroelastomer. *Mater. Focus* **2018**, *7*, 194–206. [CrossRef]
75. Bhardwaj, N.; Kundu, S.C. Electrospinning: A fascinating fiber fabrication technique. *Biotechnol. Adv.* **2010**, *28*, 325–347. [CrossRef]
76. Sill, T.J.; von Recum, H.A. Electrospinning: Applications in drug delivery and tissue engineering. *Biomaterials* **2008**, *29*, 1989–2006. [CrossRef]
77. Braghirolli, D.I.; Steffens, D.; Pranke, P. Electrospinning for regenerative medicine: A review of the main topics. *Drug Discov. Today* **2014**, *19*, 743–753. [CrossRef]
78. Badhe, Y.; Balasubramanian, K. Nanoencapsulated core and shell electrospun fibers of resorcinol formaldehyde. *Ind. Eng. Chem. Res.* **2015**, *54*, 7614–7622. [CrossRef]
79. Bhalara, P.D.; Balasubramanian, K.; Banerjee, B.S. Spider–web textured electrospun composite of graphene for sorption of Hg (II) ions. *Mater. Focus* **2015**, *4*, 154–163. [CrossRef]
80. Ramakrishna, S.; Fujihara, K.; Teo, W.-E.; Yong, T.; Ma, Z.; Ramaseshan, R. Electrospun nanofibers: Solving global issues. *Mater. Today* **2006**, *9*, 40–50. [CrossRef]
81. Malik, R.; Garg, T.; Goyal, A.K.; Rath, G. Polymeric nanofibers: Targeted gastro-retentive drug delivery systems. *J. Drug Target.* **2015**, *23*, 109–124. [CrossRef]
82. Kar, K.K.; Rana, S.; Pandey, J. *Handbook of Polymer Nanocomposites Processing, Performance and Application*; Springer: Berlin/Heidelberg, Germany, 2015.
83. Lee, J.; Kwon, H.; Seo, J.; Shin, S.; Koo, J.H.; Pang, C.; Son, S.; Kim, J.H.; Jang, Y.H.; Kim, D.E. Conductive fiber-based ultrasensitive textile pressure sensor for wearable electronics. *Adv. Mater.* **2015**, *27*, 2433–2439. [CrossRef]
84. Topuz, F.; Uyar, T. Electrospinning of gelatin with tunable fiber morphology from round to flat/ribbon. *Mater. Sci. Eng. C* **2017**, *80*, 371–378. [CrossRef]
85. Ki, C.S.; Baek, D.H.; Gang, K.D.; Lee, K.H.; Um, I.C.; Park, Y.H. Characterization of gelatin nanofiber prepared from gelatin–formic acid solution. *Polymer* **2005**, *46*, 5094–5102. [CrossRef]
86. Nadri, S.; Nasehi, F.; Barati, G. Effect of parameters on the quality of core-shell fibrous scaffold for retinal differentiation of conjunctiva mesenchymal stem cells. *J. Biomed. Mater. Res. Part A* **2017**, *105*, 189–197. [CrossRef]
87. Liu, Q.; Wang, Y.; Dai, L.; Yao, J. Scalable Fabrication of Nanoporous Carbon Fiber Films as Bifunctional Catalytic Electrodes for Flexible Zn-Air Batteries. *Adv. Mater.* **2016**, *28*, 3000–3006. [CrossRef]
88. Bedane, A.H.; Eić, M.; Farmahini-Farahani, M.; Xiao, H. Theoretical modeling of water vapor transport in cellulose-based materials. *Cellulose* **2016**, *23*, 1537–1552. [CrossRef]
89. Ambekar, R.S.; Kandasubramanian, B. Advancements in nanofibers for wound dressing: A review. *Eur. Polym. J.* **2019**, *117*, 304–336. [CrossRef]
90. Pillay, V.; Dott, C.; Choonara, Y.E.; Tyagi, C.; Tomar, L.; Kumar, P.; du Toit, L.C.; Ndesendo, V.M.K. A Review of the Effect of Processing Variables on the Fabrication of Electrospun Nanofibers for Drug Delivery Applications. *J. Nanomater.* **2013**, *2013*, 789289. [CrossRef]
91. Chou, S.-F.; Carson, D.; Woodrow, K.A. Current strategies for sustaining drug release from electrospun nanofibers. *J. Control. Release* **2015**, *220*, 584–591. [CrossRef]
92. Lu, Y.; Huang, J.; Yu, G.; Cardenas, R.; Wei, S.; Wujcik, E.K.; Guo, Z. Coaxial electrospun fibers: Applications in drug delivery and tissue engineering. *Wiley Interdiscip. Rev. Nanomed. Nanobiotechnol.* **2016**, *8*, 654–677. [CrossRef]

93. Yu, D.-G.; Li, X.-Y.; Wang, X.; Yang, J.-H.; Bligh, S.A.; Williams, G.R. Nanofibers fabricated using triaxial electrospinning as zero order drug delivery systems. *ACS Appl. Mater. Interfaces* **2015**, *7*, 18891–18897. [CrossRef]
94. Han, D.; Steckl, A.J. Triaxial electrospun nanofiber membranes for controlled dual release of functional molecules. *ACS Appl. Mater. Interfaces* **2013**, *5*, 8241–8245. [CrossRef]
95. Horst, M.; Madduri, S.; Milleret, V.; Sulser, T.; Gobet, R.; Eberli, D. A bilayered hybrid microfibrous PLGA–acellular matrix scaffold for hollow organ tissue engineering. *Biomaterials* **2013**, *34*, 1537–1545. [CrossRef]
96. Li, D.; Xia, Y. Direct fabrication of composite and ceramic hollow nanofibers by electrospinning. *Nano Lett.* **2004**, *4*, 933–938. [CrossRef]
97. Ren, B.; Fan, M.; Liu, Q.; Wang, J.; Song, D.; Bai, X. Hollow NiO nanofibers modified by citric acid and the performances as supercapacitor electrode. *Electrochim. Acta* **2013**, *92*, 197–204. [CrossRef]
98. Gupta, P.; Wilkes, G.L. Some investigations on the fiber formation by utilizing a side-by-side bicomponent electrospinning approach. *Polymer* **2003**, *44*, 6353–6359. [CrossRef]
99. Gu, B.K.; Shin, M.K.; Sohn, K.W.; Kim, S.I.; Kim, S.J.; Kim, S.-K.; Lee, H.; Park, J.S. Direct fabrication of twisted nanofibers by electrospinning. *Appl. Phys. Lett.* **2007**, *90*, 263902. [CrossRef]
100. Canejo, J.P.; Borges, J.P.; Godinho, M.H.; Brogueira, P.; Teixeira, P.I.; Terentjev, E.M. Helical twisting of electrospun liquid crystalline cellulose micro-and nanofibers. *Adv. Mater.* **2008**, *20*, 4821–4825. [CrossRef]
101. Ji, L.; Medford, A.J.; Zhang, X. Porous carbon nanofibers loaded with manganese oxide particles: Formation mechanism and electrochemical performance as energy-storage materials. *J. Mater. Chem.* **2009**, *19*, 5593–5601. [CrossRef]
102. Dayal, P.; Liu, J.; Kumar, S.; Kyu, T. Experimental and theoretical investigations of porous structure formation in electrospun fibers. *Macromolecules* **2007**, *40*, 7689–7694. [CrossRef]
103. Le Ouay, B.; Stellacci, F. Antibacterial activity of silver nanoparticles: A surface science insight. *Nano Today* **2015**, *10*, 339–354. [CrossRef]
104. Rychter, M.; Baranowska-Korczyc, A.; Lulek, J. Progress and perspectives in bioactive agent delivery via electrospun vascular grafts. *RSC Adv.* **2017**, *7*, 32164–32184. [CrossRef]
105. Jiang, S.; Chen, Y.; Duan, G.; Mei, C.; Greiner, A.; Agarwal, S. Electrospun nanofiber reinforced composites: A review. *Polym. Chem.* **2018**, *9*, 2685–2720. [CrossRef]
106. Hong, J.K.; Bang, J.Y.; Xu, G.; Lee, J.-H.; Kim, Y.-J.; Lee, H.-J.; Kim, H.S.; Kwon, S.-M. Thickness-controllable electrospun fibers promote tubular structure formation by endothelial progenitor cells. *Int. J. Nanomed.* **2015**, *10*, 1189.
107. Rnjak-Kovacina, J.; Weiss, A.S. Increasing the pore size of electrospun scaffolds. *Tissue Eng. Part B Rev.* **2011**, *17*, 365–372. [CrossRef]
108. Leong, M.F.; Rasheed, M.Z.; Lim, T.C.; Chian, K.S. In vitro cell infiltration and in vivo cell infiltration and vascularization in a fibrous, highly porous poly (D, L-lactide) scaffold fabricated by cryogenic electrospinning technique. *J. Biomed. Mater. Res. Part A* **2009**, *91*, 231–240. [CrossRef]
109. Telemeco, T.; Ayres, C.; Bowlin, G.; Wnek, G.; Boland, E.; Cohen, N.; Baumgarten, C.; Mathews, J.; Simpson, D. Regulation of cellular infiltration into tissue engineering scaffolds composed of submicron diameter fibrils produced by electrospinning. *Acta Biomater.* **2005**, *1*, 377–385. [CrossRef]
110. Rnjak-Kovacina, J.; Wise, S.G.; Li, Z.; Maitz, P.K.; Young, C.J.; Wang, Y.; Weiss, A.S. Tailoring the porosity and pore size of electrospun synthetic human elastin scaffolds for dermal tissue engineering. *Biomaterials* **2011**, *32*, 6729–6736. [CrossRef]
111. Álvarez, Z.; Castaño, O.; Castells, A.A.; Mateos-Timoneda, M.A.; Planell, J.A.; Engel, E.; Alcántara, S. Neurogenesis and vascularization of the damaged brain using a lactate-releasing biomimetic scaffold. *Biomaterials* **2014**, *35*, 4769–4781. [CrossRef]
112. Kang, L.; Jia, W.; Li, M.; Wang, Q.; Wang, C.; Liu, Y.; Wang, X.; Jin, L.; Jiang, J.; Gu, G. Hyaluronic acid oligosaccharide-modified collagen nanofibers as vascular tissue-engineered scaffold for promoting endothelial cell proliferation. *Carbohydr. Polym.* **2019**, *223*, 115106. [CrossRef] [PubMed]
113. Park, S.M.; Lee, K.-P.; Huh, M.-I.; Eom, S.; Park, B.-U.; Kim, K.H.; Park, D.H.; Kim, D.S.; Kim, H.K. Development of an in vitro 3D choroidal neovascularization model using chemically induced hypoxia through an ultra-thin, free-standing nanofiber membrane. *Mater. Sci. Eng. C* **2019**, *104*, 109964. [CrossRef]

114. Wu, Y.; Qin, Y.; Wang, Z.; Wang, J.; Zhang, C.; Li, C.; Kong, D. The regeneration of macro-porous electrospun poly (ε-caprolactone) vascular graft during long-term in situ implantation. *J. Biomed. Mater. Res. Part B Appl. Biomater.* **2018**, *106*, 1618–1627. [CrossRef] [PubMed]
115. Walthers, C.M.; Nazemi, A.K.; Patel, S.L.; Wu, B.M.; Dunn, J.C. The effect of scaffold macroporosity on angiogenesis and cell survival in tissue-engineered smooth muscle. *Biomaterials* **2014**, *35*, 5129–5137. [CrossRef] [PubMed]
116. Jundziłł, A.; Pokrywczyńska, M.; Adamowicz, J.; Kowalczyk, T.; Nowacki, M.; Bodnar, M.; Marszałek, A.; Frontczak-Baniewicz, M.; Mikułowski, G.; Kloskowski, T. Vascularization potential of electrospun poly (L-lactide-co-caprolactone) scaffold: The Impact for tissue engineering. *Med. Sci. Monit. Int. Med. J. Exp. Clin. Res.* **2017**, *23*, 1540. [CrossRef]
117. Li, X.; Cho, B.; Martin, R.; Seu, M.; Zhang, C.; Zhou, Z.; Choi, J.S.; Jiang, X.; Chen, L.; Walia, G. Nanofiber-hydrogel composite–mediated angiogenesis for soft tissue reconstruction. *Sci. Transl. Med.* **2019**, *11*, eaau6210. [CrossRef]
118. Lee, J.B.; Balikov, D.A.; Yang, J.W.; Kim, K.S.; Park, H.K.; Kim, J.K.; Kwon, I.K.; Bellan, L.M.; Sung, H.-J. Cationic nanocylinders promote angiogenic activities of endothelial cells. *Polymers* **2016**, *8*, 15. [CrossRef]
119. Eghtesad, S.; Nurminskaya, M.V. Binding of pro-migratory serum factors to electrospun PLLA nano-fibers. *J. Biomater. Sci. Polym. Ed.* **2013**, *24*, 2006–2017. [CrossRef]
120. Jiang, J.; Li, Z.; Wang, H.; Wang, Y.; Carlson, M.A.; Teusink, M.J.; MacEwan, M.R.; Gu, L.; Xie, J. Expanded 3D nanofiber scaffolds: Cell penetration, neovascularization, and host response. *Adv. Healthc. Mater.* **2016**, *5*, 2993–3003. [CrossRef]
121. Wickham, A.; Sjölander, D.; Bergström, G.; Wang, E.; Rajendran, V.; Hildesjö, C.; Skoglund, K.; Nilsson, K.P.R.; Aili, D. Near-Infrared Emitting and Pro-Angiogenic Electrospun Conjugated Polymer Scaffold for Optical Biomaterial Tracking. *Adv. Funct. Mater.* **2015**, *25*, 4274–4281. [CrossRef]
122. Castellano, D.; Blanes, M.; Marco, B.; Cerrada, I.; Ruiz-Saurí, A.; Pelacho, B.; Arana, M.; Montero, J.A.; Cambra, V.; Prosper, F. A comparison of electrospun polymers reveals poly (3-hydroxybutyrate) fiber as a superior scaffold for cardiac repair. *Stem Cells Dev.* **2014**, *23*, 1479–1490. [CrossRef]
123. Xu, H.; Li, H.; Ke, Q.; Chang, J. An anisotropically and heterogeneously aligned patterned electrospun scaffold with tailored mechanical property and improved bioactivity for vascular tissue engineering. *ACS Appl. Mater. Interfaces* **2015**, *7*, 8706–8718. [CrossRef]
124. Castellano, D.; Sanchis, A.; Blanes, M.; Pérez del Caz, M.D.; Ruiz-Saurí, A.; Piquer-Gil, M.; Pelacho, B.; Marco, B.; Garcia, N.; Ontoria-Oviedo, I. Electrospun poly (hydroxybutyrate) scaffolds promote engraftment of human skin equivalents via macrophage M2 polarization and angiogenesis. *J. Tissue Eng. Regen. Med.* **2018**, *12*, e983–e994. [CrossRef]
125. Gombotz, W.R.; Pettit, D.K. Biodegradable polymers for protein and peptide drug delivery. *Bioconjugate Chem.* **1995**, *6*, 332–351. [CrossRef]
126. Zamani, M.; Prabhakaran, M.P.; Ramakrishna, S. Advances in drug delivery via electrospun and electrosprayed nanomaterials. *Int. J. Nanomed.* **2013**, *8*, 2997.
127. Yoo, H.S.; Kim, T.G.; Park, T.G. Surface-functionalized electrospun nanofibers for tissue engineering and drug delivery. *Adv. Drug Deliv. Rev.* **2009**, *61*, 1033–1042. [CrossRef]
128. Li, Z.; Song, L.; Huang, X.; Wang, H.; Shao, H.; Xie, M.; Xu, Y.; Zhang, Y. Tough and VEGF-releasing scaffolds composed of artificial silk fibroin mats and a natural acellular matrix. *Rsc Adv.* **2015**, *5*, 16748–16758. [CrossRef]
129. Liao, I.-C.; Leong, K.W. Efficacy of engineered FVIII-producing skeletal muscle enhanced by growth factor-releasing co-axial electrospun fibers. *Biomaterials* **2011**, *32*, 1669–1677. [CrossRef]
130. Zigdon-Giladi, H.; Khutaba, A.; Elimelech, R.; Machtei, E.E.; Srouji, S. VEGF release from a polymeric nanofiber scaffold for improved angiogenesis. *J. Biomed. Mater. Res. Part A* **2017**, *105*, 2712–2721. [CrossRef]
131. Jiang, Y.-C.; Wang, X.-F.; Xu, Y.-Y.; Qiao, Y.-H.; Guo, X.; Wang, D.-F.; Li, Q.; Turng, L.-S. Polycaprolactone nanofibers containing vascular endothelial growth factor-encapsulated gelatin particles enhance mesenchymal stem cell differentiation and angiogenesis of endothelial cells. *Biomacromolecules* **2018**, *19*, 3747–3753. [CrossRef]
132. Zhang, H.; Jia, X.; Han, F.; Zhao, J.; Zhao, Y.; Fan, Y.; Yuan, X. Dual-delivery of VEGF and PDGF by double-layered electrospun membranes for blood vessel regeneration. *Biomaterials* **2013**, *34*, 2202–2212. [CrossRef]

133. Lai, H.-J.; Kuan, C.-H.; Wu, H.-C.; Tsai, J.-C.; Chen, T.-M.; Hsieh, D.-J.; Wang, T.-W. Tailored design of electrospun composite nanofibers with staged release of multiple angiogenic growth factors for chronic wound healing. *Acta Biomater.* **2014**, *10*, 4156–4166. [CrossRef]
134. Tian, L.; Prabhakaran, M.P.; Ding, X.; Kai, D.; Ramakrishna, S. Emulsion electrospun vascular endothelial growth factor encapsulated poly (l-lactic acid-co-ε-caprolactone) nanofibers for sustained release in cardiac tissue engineering. *J. Mater. Sci.* **2012**, *47*, 3272–3281. [CrossRef]
135. Nillesen, S.T.; Geutjes, P.J.; Wismans, R.; Schalkwijk, J.; Daamen, W.F.; van Kuppevelt, T.H. Increased angiogenesis and blood vessel maturation in acellular collagen–heparin scaffolds containing both FGF2 and VEGF. *Biomaterials* **2007**, *28*, 1123–1131. [CrossRef]
136. Guo, X.; Elliott, C.G.; Li, Z.; Xu, Y.; Hamilton, D.W.; Guan, J. Creating 3D angiogenic growth factor gradients in fibrous constructs to guide fast angiogenesis. *Biomacromolecules* **2012**, *13*, 3262–3271. [CrossRef]
137. Yang, Y.; Xia, T.; Zhi, W.; Wei, L.; Weng, J.; Zhang, C.; Li, X. Promotion of skin regeneration in diabetic rats by electrospun core-sheath fibers loaded with basic fibroblast growth factor. *Biomaterials* **2011**, *32*, 4243–4254. [CrossRef]
138. Zhu, X.H.; Tabata, Y.; Wang, C.-H.; Tong, Y.W. Delivery of basic fibroblast growth factor from gelatin microsphere scaffold for the growth of human umbilical vein endothelial cells. *Tissue Eng. Part A* **2008**, *14*, 1939–1947. [CrossRef]
139. Jin, Q.; Wei, G.; Lin, Z.; Sugai, J.V.; Lynch, S.E.; Ma, P.X.; Giannobile, W.V. Nanofibrous scaffolds incorporating PDGF-BB microspheres induce chemokine expression and tissue neogenesis in vivo. *PLoS ONE* **2008**, *3*, e1729. [CrossRef]
140. Roy, H.; Bhardwaj, S.; Ylä-Herttuala, S. Biology of vascular endothelial growth factors. *FEBS Lett.* **2006**, *580*, 2879–2887. [CrossRef]
141. Senger, D.R.; Galli, S.J.; Dvorak, A.M.; Perruzzi, C.A.; Harvey, V.S.; Dvorak, H.F. Tumor cells secrete a vascular permeability factor that promotes accumulation of ascites fluid. *Science* **1983**, *219*, 983–985. [CrossRef]
142. Bouïs, D.; Kusumanto, Y.; Meijer, C.; Mulder, N.H.; Hospers, G.A. A review on pro-and anti-angiogenic factors as targets of clinical intervention. *Pharm. Res.* **2006**, *53*, 89–103. [CrossRef]
143. DeVolder, R.J.; Bae, H.; Lee, J.; Kong, H. Directed blood vessel growth using an angiogenic microfiber/microparticle composite patch. *Adv. Mater.* **2011**, *23*, 3139–3143. [CrossRef]
144. Clapp, C.; Thebault, S.; Jeziorski, M.C.; Martinez De la Escalera, G. Peptide hormone regulation of angiogenesis. *Physiol. Rev.* **2009**, *89*, 1177–1215. [CrossRef]
145. Satish, A.; Korrapati, P.S. Nanofiber-Mediated Sustained Delivery of Triiodothyronine: Role in Angiogenesis. *AAPS PharmSciTech* **2019**, *20*, 110. [CrossRef]
146. Gasowska, K.; Naumnik, B.; Klejna, K.; Myśliwiec, M. The influence of unfractionated and low-molecular weight heparins on the properties of human umbilical vein endothelial cells (HUVEC). *Folia Histochem. Cytobiol.* **2009**, *47*, 17–23. [CrossRef]
147. Kuang, H.; Yang, S.; Wang, Y.; He, Y.; Ye, K.; Hu, J.; Shen, W.; Morsi, Y.; Lu, S.; Mo, X. Electrospun Bilayer Composite Vascular Graft with an Inner Layer Modified by Polyethylene Glycol and Haparin to Regenerate the Blood Vessel. *J. Biomed. Nanotechnol.* **2019**, *15*, 77–84. [CrossRef]
148. Pitarresi, G.; Fiorica, C.; Palumbo, F.S.; Rigogliuso, S.; Ghersi, G.; Giammona, G. Heparin functionalized polyaspartamide/polyester scaffold for potential blood vessel regeneration. *J. Biomed. Mater. Res. Part A* **2014**, *102*, 1334–1341. [CrossRef]
149. Ahangari, N.; Kargozar, S.; Ghayour-Mobarhan, M.; Baino, F.; Pasdar, A.; Sahebkar, A.; Ferns, G.A.; Kim, H.W.; Mozafari, M. Curcumin in tissue engineering: A traditional remedy for modern medicine. *Biofactors* **2019**, *45*, 135–151. [CrossRef]
150. Hu, Y.; Cao, S.; Chen, J.; Zhao, Y.; He, F.; Li, Q.; Zou, L.; Shi, C. Biomimetic fabrication of Icariin loaded nano hydroxyapatite reinforced bioactive porous scaffolds for bone regeneration. *Chem. Eng. J.* **2020**, *394*, 124895. [CrossRef]
151. Shefa, A.A.; Sultana, T.; Park, M.K.; Lee, S.Y.; Gwon, J.-G.; Lee, B.-T. Curcumin incorporation into an oxidized cellulose nanofiber-polyvinyl alcohol hydrogel system promotes wound healing. *Mater. Des.* **2020**, *186*, 108313. [CrossRef]
152. Rubio-Elizalde, I.; Bernáldez-Sarabia, J.; Moreno-Ulloa, A.; Vilanova, C.; Juárez, P.; Licea-Navarro, A.; Castro-Ceseña, A.B. Scaffolds based on alginate-PEG methyl ether methacrylate-Moringa oleifera-Aloe vera for wound healing applications. *Carbohydr. Polym.* **2019**, *206*, 455–467. [CrossRef]

153. Chung, B.-H.; Kim, J.-D.; Kim, C.-K.; Kim, J.H.; Won, M.-H.; Lee, H.-S.; Dong, M.-S.; Ha, K.-S.; Kwon, Y.-G.; Kim, Y.-M. Icariin stimulates angiogenesis by activating the MEK/ERK-and PI3K/Akt/eNOS-dependent signal pathways in human endothelial cells. *Biochem. Biophys. Res. Commun.* **2008**, *376*, 404–408. [CrossRef]
154. Basak, S.; Srinivas, V.; Mallepogu, A.; Duttaroy, A.K. Curcumin stimulates angiogenesis through VEGF and expression of HLA-G in first-trimester human placental trophoblasts. *Cell Biol. Int.* **2020**, *44*, 1237–1251. [CrossRef]
155. Hosseini, A.; Rasmi, Y.; Rahbarghazi, R.; Aramwit, P.; Daeihassani, B.; Saboory, E. Curcumin modulates the angiogenic potential of human endothelial cells via FAK/P-38 MAPK signaling pathway. *Gene* **2019**, *688*, 7–12. [CrossRef]
156. Wang, T.-Y.; Chen, J.-X. Effects of Curcumin on Vessel Formation Insight into the Pro- and Antiangiogenesis of Curcumin. *Evid. Based Complementary Altern. Med.* **2019**, *2019*, 1390795. [CrossRef]
157. Zhu, L.; Liu, X.; Du, L.; Jin, Y. Preparation of asiaticoside-loaded coaxially electrospinning nanofibers and their effect on deep partial-thickness burn injury. *Biomed. Pharmacother.* **2016**, *83*, 33–40. [CrossRef]
158. Diaz-Gomez, L.; Alvarez-Lorenzo, C.; Concheiro, A.; Silva, M.; Dominguez, F.; Sheikh, F.A.; Cantu, T.; Desai, R.; Garcia, V.L.; Macossay, J. Biodegradable electrospun nanofibers coated with platelet-rich plasma for cell adhesion and proliferation. *Mater. Sci. Eng. C* **2014**, *40*, 180–188. [CrossRef]
159. Cheng, G.; Ma, X.; Li, J.; Cheng, Y.; Cao, Y.; Wang, Z.; Shi, X.; Du, Y.; Deng, H.; Li, Z. Incorporating platelet-rich plasma into coaxial electrospun nanofibers for bone tissue engineering. *Int. J. Pharm.* **2018**, *547*, 656–666. [CrossRef]
160. Zhao, L.; Ma, S.; Pan, Y.; Zhang, Q.; Wang, K.; Song, D.; Wang, X.; Feng, G.; Liu, R.; Xu, H. Functional modification of fibrous PCL scaffolds with fusion protein VEGF-HGFI enhanced cellularization and vascularization. *Adv. Healthc. Mater.* **2016**, *5*, 2376–2385. [CrossRef]
161. John, J.V.; Choksi, M.; Chen, S.; Boda, S.K.; Su, Y.; McCarthy, A.; Teusink, M.J.; Reinhardt, R.A.; Xie, J. Tethering peptides onto biomimetic and injectable nanofiber microspheres to direct cellular response. *Nanomed. Nanotechnol. Biol. Med.* **2019**, *22*, 102081. [CrossRef]
162. Deng, A.; Yang, Y.; Du, S.; Yang, S. Electrospinning of in situ crosslinked recombinant human collagen peptide/chitosan nanofibers for wound healing. *Biomater. Sci.* **2018**, *6*, 2197–2208. [CrossRef]
163. Rameshbabu, A.P.; Datta, S.; Bankoti, K.; Subramani, E.; Chaudhury, K.; Lalzawmliana, V.; Nandi, S.K.; Dhara, S. Polycaprolactone nanofibers functionalized with placental derived extracellular matrix for stimulating wound healing activity. *J. Mater. Chem. B* **2018**, *6*, 6767–6780. [CrossRef]
164. Zhou, Z.; Long, D.; Hsu, C.-C.; Liu, H.; Chen, L.; Slavin, B.; Lin, H.; Li, X.; Tang, J.; Yiu, S. Nanofiber-reinforced decellularized amniotic membrane improves limbal stem cell transplantation in a rabbit model of corneal epithelial defect. *Acta Biomater.* **2019**, *97*, 310–320. [CrossRef]
165. Jaganathan, S.K.; Mani, M.P.; Khudzari, A.Z.M. Electrospun combination of peppermint oil and copper sulphate with conducive physico-chemical properties for wound dressing applications. *Polymers* **2019**, *11*, 586. [CrossRef]
166. Jaganathan, S.K.; Mani, M.P. Electrospun polyurethane nanofibrous composite impregnated with metallic copper for wound-healing application. *3 Biotech* **2018**, *8*, 327. [CrossRef]
167. Gholipourmalekabadi, M.; Samadikuchaksaraei, A.; Seifalian, A.M.; Urbanska, A.M.; Ghanbarian, H.; Hardy, J.G.; Omrani, M.D.; Mozafari, M.; Reis, R.L.; Kundu, S.C. Silk fibroin/amniotic membrane 3D bi-layered artificial skin. *Biomed. Mater.* **2018**, *13*, 035003. [CrossRef]
168. Kargozar, S.; Baino, F.; Hamzehlou, S.; Hill, R.G.; Mozafari, M. Bioactive glasses: Sprouting angiogenesis in tissue engineering. *Trends Biotechnol.* **2018**, *36*, 430–444. [CrossRef]
169. Malhotra, A.; Habibovic, P. Calcium phosphates and angiogenesis: Implications and advances for bone regeneration. *Trends Biotechnol.* **2016**, *34*, 983–992. [CrossRef]
170. Zhai, W.; Lu, H.; Wu, C.; Chen, L.; Lin, X.; Naoki, K.; Chen, G.; Chang, J. Stimulatory effects of the ionic products from Ca–Mg–Si bioceramics on both osteogenesis and angiogenesis in vitro. *Acta Biomater.* **2013**, *9*, 8004–8014. [CrossRef]
171. Xia, L.; Yin, Z.; Mao, L.; Wang, X.; Liu, J.; Jiang, X.; Zhang, Z.; Lin, K.; Chang, J.; Fang, B. Akermanite bioceramics promote osteogenesis, angiogenesis and suppress osteoclastogenesis for osteoporotic bone regeneration. *Sci. Rep.* **2016**, *6*, 22005. [CrossRef]

172. Chen, Y.; Wang, J.; Zhu, X.; Tang, Z.; Yang, X.; Tan, Y.; Fan, Y.; Zhang, X. Enhanced effect of β-tricalcium phosphate phase on neovascularization of porous calcium phosphate ceramics: In vitro and in vivo evidence. *Acta Biomater.* **2015**, *11*, 435–448. [CrossRef]
173. Wang, J.; Qian, S.; Liu, X.; Xu, L.; Miao, X.; Xu, Z.; Cao, L.; Wang, H.; Jiang, X. M2 macrophages contribute to osteogenesis and angiogenesis on nanotubular TiO 2 surfaces. *J. Mater. Chem. B* **2017**, *5*, 3364–3376. [CrossRef] [PubMed]
174. Kargozar, S.; Baino, F.; Hamzehlou, S.; Hill, R.G.; Mozafari, M. Bioactive glasses entering the mainstream. *Drug Discov. Today* **2018**, *23*, 1700–1704. [CrossRef] [PubMed]
175. Lin, Y.; Xiao, W.; Bal, B.S.; Rahaman, M.N. Effect of copper-doped silicate 13–93 bioactive glass scaffolds on the response of MC3T3-E1 cells in vitro and on bone regeneration and angiogenesis in rat calvarial defects in vivo. *Mater. Sci. Eng. C* **2016**, *67*, 440–452. [CrossRef]
176. Kargozar, S.; Lotfibakhshaiesh, N.; Ai, J.; Samadikuchaksaraie, A.; Hill, R.G.; Shah, P.A.; Milan, P.B.; Mozafari, M.; Fathi, M.; Joghataei, M.T. Synthesis, physico-chemical and biological characterization of strontium and cobalt substituted bioactive glasses for bone tissue engineering. *J. Non-Cryst. Solids* **2016**, *449*, 133–140. [CrossRef]
177. Weng, L.; Boda, S.K.; Teusink, M.J.; Shuler, F.D.; Li, X.; Xie, J. Binary doping of strontium and copper enhancing osteogenesis and angiogenesis of bioactive glass nanofibers while suppressing osteoclast activity. *ACS Appl. Mater. Interfaces* **2017**, *9*, 24484–24496. [CrossRef] [PubMed]
178. Kargozar, S.; Mozafari, M.; Hill, R.G.; Brouki Milan, P.; Taghi Joghataei, M.; Hamzehlou, S.; Baino, F. Synergistic combination of bioactive glasses and polymers for enhanced bone tissue regeneration. *Mater. Today Proc.* **2018**, *5*, 15532–15539. [CrossRef]
179. Deliormanlı, A.M. Electrospun cerium and gallium-containing silicate based 13-93 bioactive glass fibers for biomedical applications. *Ceram. Int.* **2016**, *42*, 897–906. [CrossRef]
180. Serio, F.; Miola, M.; Vernè, E.; Pisignano, D.; Boccaccini, A.R.; Liverani, L. Electrospun Filaments Embedding Bioactive Glass Particles with Ion Release and Enhanced Mineralization. *Nanomaterials* **2019**, *9*, 182. [CrossRef]
181. Sachot, N.; Roguska, A.; Planell, J.A.; Lewandowska, M.; Engel, E.; Castaño, O. Fast-degrading PLA/ORMOGLASS fibrous composite scaffold leads to a calcium-rich angiogenic environment. *Int. J. Nanomed.* **2017**, *12*, 4901. [CrossRef]
182. Shamosi, A.; Mehrabani, D.; Azami, M.; Ebrahimi-Barough, S.; Siavashi, V.; Ghanbari, H.; Sharifi, E.; Roozafzoon, R.; Ai, J. Differentiation of human endometrial stem cells into endothelial-like cells on gelatin/chitosan/bioglass nanofibrous scaffolds. *Artif. Cells Nanomed. Biotechnol.* **2017**, *45*, 163–173. [CrossRef]
183. Oliveira, H.; Catros, S.; Boiziau, C.; Siadous, R.; Marti-Munoz, J.; Bareille, R.; Rey, S.; Castano, O.; Planell, J.; Amédée, J. The proangiogenic potential of a novel calcium releasing biomaterial: Impact on cell recruitment. *Acta Biomater.* **2016**, *29*, 435–445. [CrossRef]
184. Bose, S.; Fielding, G.; Tarafder, S.; Bandyopadhyay, A. Understanding of dopant-induced osteogenesis and angiogenesis in calcium phosphate ceramics. *Trends Biotechnol.* **2013**, *31*, 594–605. [CrossRef]
185. Song, Y.; Wu, H.; Gao, Y.; Li, J.; Lin, K.; Liu, B.; Lei, X.; Cheng, P.; Zhang, S.; Wang, Y. Zinc Silicate/Nano-Hydroxyapatite/Collagen Scaffolds Promote Angiogenesis and Bone Regeneration via the p38 MAPK Pathway in Activated Monocytes. *ACS Appl. Mater. Interfaces* **2020**, *12*, 16058–16075. [CrossRef]
186. Wang, M.; Yu, Y.; Dai, K.; Ma, Z.; Liu, Y.; Wang, J.; Liu, C. Improved osteogenesis and angiogenesis of magnesium-doped calcium phosphate cement via macrophage immunomodulation. *Biomater. Sci.* **2016**, *4*, 1574–1583. [CrossRef]
187. Sun, W.; Zhou, Y.; Zhang, X.; Xia, W.; Xu, Y.; Lin, K. Injectable nano-structured silicon-containing hydroxyapatite microspheres with enhanced osteogenic differentiation and angiogenic factor expression. *Ceram. Int.* **2018**, *44*, 20457–20464. [CrossRef]
188. Ye, H.; Zhu, J.; Deng, D.; Jin, S.; Li, J.; Man, Y. Enhanced osteogenesis and angiogenesis by PCL/chitosan/Sr-doped calcium phosphate electrospun nanocomposite membrane for guided bone regeneration. *J. Biomater. Sci. Polym. Ed.* **2019**, *30*, 1505–1522. [CrossRef]
189. Kang, B.-J.; Kim, H.; Lee, S.K.; Kim, J.; Shen, Y.; Jung, S.; Kang, K.-S.; Im, S.G.; Lee, S.Y.; Choi, M.; et al. Umbilical-cord-blood-derived mesenchymal stem cells seeded onto fibronectin-immobilized polycaprolactone nanofiber improve cardiac function. *Acta Biomater.* **2014**, *10*, 3007–3017. [CrossRef]

190. Mukherjee, S.; Darzi, S.; Paul, K.; Cousins, F.L.; Werkmeister, J.A.; Gargett, C.E. Electrospun Nanofiber Meshes With Endometrial MSCs Modulate Foreign Body Response by Increased Angiogenesis, Matrix Synthesis, and Anti-Inflammatory Gene Expression in Mice: Implication in Pelvic Floor. *Front. Pharmacol.* **2020**, *11*, 353. [CrossRef]
191. Kook, Y.-M.; Kim, H.; Kim, S.; Heo, C.Y.; Park, M.H.; Lee, K.; Koh, W.-G. Promotion of vascular morphogenesis of endothelial cells co-cultured with human adipose-derived mesenchymal stem cells using polycaprolactone/gelatin nanofibrous scaffolds. *Nanomaterials* **2018**, *8*, 117. [CrossRef]
192. Carmeliet, P. Angiogenesis in health and disease. *Nat. Med.* **2003**, *9*, 653–660. [CrossRef] [PubMed]
193. Rehman, J.; Li, J.; Orschell, C.M.; March, K.L. Peripheral blood "endothelial progenitor cells" are derived from monocyte/macrophages and secrete angiogenic growth factors. *Circulation* **2003**, *107*, 1164–1169. [CrossRef] [PubMed]
194. Kalka, C.; Masuda, H.; Takahashi, T.; Kalka-Moll, W.M.; Silver, M.; Kearney, M.; Li, T.; Isner, J.M.; Asahara, T. Transplantation of ex vivo expanded endothelial progenitor cells for therapeutic neovascularization. *Proc. Natl. Acad. Sci. USA* **2000**, *97*, 3422–3427. [CrossRef] [PubMed]
195. Coultas, L.; Chawengsaksophak, K.; Rossant, J. Endothelial cells and VEGF in vascular development. *Nature* **2005**, *438*, 937–945. [CrossRef] [PubMed]
196. Bian, S.; Zhang, L.; Duan, L.; Wang, X.; Min, Y.; Yu, H. Extracellular vesicles derived from human bone marrow mesenchymal stem cells promote angiogenesis in a rat myocardial infarction model. *J. Mol. Med.* **2014**, *92*, 387–397. [CrossRef]
197. Grange, C.; Tapparo, M.; Collino, F.; Vitillo, L.; Damasco, C.; Deregibus, M.C.; Tetta, C.; Bussolati, B.; Camussi, G. Microvesicles released from human renal cancer stem cells stimulate angiogenesis and formation of lung premetastatic niche. *Cancer Res.* **2011**, *71*, 5346–5356. [CrossRef]
198. Zhu, Y.; Zhang, J.; Hu, X.; Wang, Z.; Wu, S.; Yi, Y. Extracellular vesicles derived from human adipose-derived stem cells promote the exogenous angiogenesis of fat grafts via the let-7/AGO1/VEGF signalling pathway. *Sci. Rep.* **2020**, *10*, 5313. [CrossRef]
199. Deregibus, M.C.; Cantaluppi, V.; Calogero, R.; Lo Iacono, M.; Tetta, C.; Biancone, L.; Bruno, S.; Bussolati, B.; Camussi, G. Endothelial progenitor cell–derived microvesicles activate an angiogenic program in endothelial cells by a horizontal transfer of mRNA. *Blood J. Am. Soc. Hematol.* **2007**, *110*, 2440–2448. [CrossRef]
200. Braghirolli, D.; Helfer, V.; Chagastelles, P.; Dalberto, T.; Gamba, D.; Pranke, P. Electrospun scaffolds functionalized with heparin and vascular endothelial growth factor increase the proliferation of endothelial progenitor cells. *Biomed. Mater.* **2017**, *12*, 025003. [CrossRef]
201. Dikici, S.; Claeyssens, F.; MacNeil, S. Pre-Seeding of Simple Electrospun Scaffolds with a Combination of Endothelial Cells and Fibroblasts Strongly Promotes Angiogenesis. *Tissue Eng. Regen. Med.* **2020**, *17*, 445–458. [CrossRef]
202. Wang, Z.; Wu, Y.; Wang, J.; Zhang, C.; Yan, H.; Zhu, M.; Wang, K.; Li, C.; Xu, Q.; Kong, D. Effect of resveratrol on modulation of endothelial cells and macrophages for rapid vascular regeneration from electrospun poly (ε-caprolactone) scaffolds. *ACS Appl. Mater. Interfaces* **2017**, *9*, 19541–19551. [CrossRef] [PubMed]
203. Chen, Y.C.; Lin, R.Z.; Qi, H.; Yang, Y.; Bae, H.; Melero-Martin, J.M.; Khademhosseini, A. Functional human vascular network generated in photocrosslinkable gelatin methacrylate hydrogels. *Adv. Funct. Mater.* **2012**, *22*, 2027–2039. [CrossRef] [PubMed]
204. Hong, S.; Kang, E.Y.; Byeon, J.; Jung, S.-h.; Hwang, C. Embossed membranes with vascular patterns guide vascularization in a 3D tissue model. *Polymers* **2019**, *11*, 792. [CrossRef] [PubMed]
205. Pill, K.; Hofmann, S.; Redl, H.; Holnthoner, W. Vascularization mediated by mesenchymal stem cells from bone marrow and adipose tissue: A comparison. *Cell Regen.* **2015**, *4*, 8. [CrossRef] [PubMed]
206. Su, N.; Gao, P.-L.; Wang, K.; Wang, J.-Y.; Zhong, Y.; Luo, Y. Fibrous scaffolds potentiate the paracrine function of mesenchymal stem cells: A new dimension in cell-material interaction. *Biomaterials* **2017**, *141*, 74–85. [CrossRef]
207. Chen, J.; Zhan, Y.; Wang, Y.; Han, D.; Tao, B.; Luo, Z.; Ma, S.; Wang, Q.; Li, X.; Fan, L. Chitosan/silk fibroin modified nanofibrous patches with mesenchymal stem cells prevent heart remodeling post-myocardial infarction in rats. *Acta Biomater.* **2018**, *80*, 154–168. [CrossRef]
208. Wang, T.; Zhai, Y.; Nuzzo, M.; Yang, X.; Yang, Y.; Zhang, X. Layer-by-layer nanofiber-enabled engineering of biomimetic periosteum for bone repair and reconstruction. *Biomaterials* **2018**, *182*, 279–288. [CrossRef]

209. Srouji, S.; Kizhner, T.; Suss-Tobi, E.; Livne, E.; Zussman, E. 3-D Nanofibrous electrospun multilayered construct is an alternative ECM mimicking scaffold. *J. Mater. Sci. Mater. Med.* **2008**, *19*, 1249–1255. [CrossRef]
210. Rufaihah, A.J.; Huang, N.F.; Jamé, S.; Lee, J.C.; Nguyen, H.N.; Byers, B.; De, A.; Okogbaa, J.; Rollins, M.; Reijo-Pera, R. Endothelial cells derived from human iPSCS increase capillary density and improve perfusion in a mouse model of peripheral arterial disease. *Arterioscler. Thromb. Vasc. Biol.* **2011**, *31*, e72–e79. [CrossRef]
211. Li, J.; Huang, N.F.; Zou, J.; Laurent, T.J.; Lee, J.C.; Okogbaa, J.; Cooke, J.P.; Ding, S. Conversion of human fibroblasts to functional endothelial cells by defined factors. *Arterioscler. Thromb. Vasc. Biol.* **2013**, *33*, 1366–1375. [CrossRef]
212. Lai, W.-H.; Ho, J.C.; Chan, Y.-C.; Ng, J.H.; Au, K.-W.; Wong, L.-Y.; Siu, C.-W.; Tse, H.-F. Attenuation of hind-limb ischemia in mice with endothelial-like cells derived from different sources of human stem cells. *PLoS ONE* **2013**, *8*, e57876. [CrossRef]
213. Tan, R.P.; Chan, A.H.; Lennartsson, K.; Miravet, M.M.; Lee, B.S.; Rnjak-Kovacina, J.; Clayton, Z.E.; Cooke, J.P.; Ng, M.K.; Patel, S. Integration of induced pluripotent stem cell-derived endothelial cells with polycaprolactone/gelatin-based electrospun scaffolds for enhanced therapeutic angiogenesis. *Stem Cell Res. Ther.* **2018**, *9*, 70. [CrossRef]
214. Sheikh, I.; Tchekanov, G.; Krum, D.; Hare, J.; Djelmami-Hani, M.; Maddikunta, R.; Mortada, M.E.; Karakozov, P.; Baibekov, I.; Hauck, J. Effect of electrical stimulation on arteriogenesis and angiogenesis after bilateral femoral artery excision in the rabbit hind-limb ischemia model. *Vasc. Endovasc. Surg.* **2005**, *39*, 257–265. [CrossRef] [PubMed]
215. Hang, J.; Kong, L.; Gu, J.; Adair, T. VEGF gene expression is upregulated in electrically stimulated rat skeletal muscle. *Am. J. Physiol. -Heart Circ. Physiol.* **1995**, *269*, H1827–H1831. [CrossRef]
216. McLean, N.A.; Verge, V.M. Dynamic impact of brief electrical nerve stimulation on the neural immune axis—Polarization of macrophages toward a pro-repair phenotype in demyelinated peripheral nerve. *Glia* **2016**, *64*, 1546–1561. [CrossRef] [PubMed]
217. Ud-Din, S.; Sebastian, A.; Giddings, P.; Colthurst, J.; Whiteside, S.; Morris, J.; Nuccitelli, R.; Pullar, C.; Baguneid, M.; Bayat, A. Angiogenesis is induced and wound size is reduced by electrical stimulation in an acute wound healing model in human skin. *PLoS ONE* **2015**, *10*, e0124502. [CrossRef] [PubMed]
218. Sebastian, A.; Syed, F.; Perry, D.; Balamurugan, V.; Colthurst, J.; Chaudhry, I.H.; Bayat, A. Acceleration of cutaneous healing by electrical stimulation: Degenerate electrical waveform down-regulates inflammation, up-regulates angiogenesis and advances remodeling in temporal punch biopsies in a human volunteer study. *Wound Repair Regen.* **2011**, *19*, 693–708. [CrossRef]
219. Bai, H.; Forrester, J.V.; Zhao, M. DC electric stimulation upregulates angiogenic factors in endothelial cells through activation of VEGF receptors. *Cytokine* **2011**, *55*, 110–115. [CrossRef]
220. Zhao, M.; Bai, H.; Wang, E.; Forrester, J.V.; McCaig, C.D. Electrical stimulation directly induces pre-angiogenic responses in vascular endothelial cells by signaling through VEGF receptors. *J. Cell Sci.* **2004**, *117*, 397–405. [CrossRef]
221. Kim, I.S.; Song, J.K.; Song, Y.M.; Cho, T.H.; Lee, T.H.; Lim, S.S.; Kim, S.J.; Hwang, S.J. Novel effect of biphasic electric current on in vitro osteogenesis and cytokine production in human mesenchymal stromal cells. *Tissue Eng. Part A* **2009**, *15*, 2411–2422. [CrossRef]
222. Beugels, J.; Molin, D.G.M.; Ophelders, D.R.M.G.; Rutten, T.; Kessels, L.; Kloosterboer, N.; Grzymala, A.A.P.d.; Kramer, B.W.W.; van der Hulst, R.R.W.J.; Wolfs, T.G.A.M. Electrical stimulation promotes the angiogenic potential of adipose-derived stem cells. *Sci. Rep.* **2019**, *9*, 12076. [CrossRef]
223. Rackauskas, G.; Saygili, E.; Rana, O.R.; Saygili, E.; Gemein, C.; Laucevicius, A.; Aidietis, A.; Marinskis, G.; Serpytis, P.; Plisiene, J. Subthreshold high-frequency electrical field stimulation induces VEGF expression in cardiomyocytes. *Cell Transplant.* **2015**, *24*, 1653–1659. [CrossRef] [PubMed]
224. Kim, I.S.; Song, J.K.; Zhang, Y.L.; Lee, T.H.; Cho, T.H.; Song, Y.M.; Kim, S.J.; Hwang, S.J. Biphasic electric current stimulates proliferation and induces VEGF production in osteoblasts. *BBA-Mol. Cell Res.* **2006**, *1763*, 907–916. [CrossRef] [PubMed]
225. Qu, J.; Zhao, X.; Liang, Y.; Xu, Y.; Ma, P.X.; Guo, B. Degradable conductive injectable hydrogels as novel antibacterial, anti-oxidant wound dressings for wound healing. *Chem. Eng. J.* **2019**, *362*, 548–560. [CrossRef]

226. Liang, Y.; Zhao, X.; Hu, T.; Han, Y.; Guo, B. Mussel-inspired, antibacterial, conductive, antioxidant, injectable composite hydrogel wound dressing to promote the regeneration of infected skin. *J. Colloid Interface Sci.* **2019**, *556*, 514–528. [CrossRef]
227. Mihardja, S.S.; Sievers, R.E.; Lee, R.J. The effect of polypyrrole on arteriogenesis in an acute rat infarct model. *Biomaterials* **2008**, *29*, 4205–4210. [CrossRef]
228. Sekuła, M.; Domalik-Pyzik, P.; Morawska-Chochół, A.; Bobis-Wozowicz, S.; Karnas, E.; Noga, S.; Boruczkowski, D.; Adamiak, M.; Madeja, Z.; Chłopek, J. Polylactide-and polycaprolactone-based substrates enhance angiogenic potential of human umbilical cord-derived mesenchymal stem cells in vitro-implications for cardiovascular repair. *Mater. Sci. Eng. C* **2017**, *77*, 521–533. [CrossRef]
229. Streeter, B.W.; Xue, J.; Xia, Y.; Davis, M.E. Electrospun Nanofiber-Based Patches for the Delivery of Cardiac Progenitor Cells. *ACS Appl. Mater. Interfaces* **2019**, *11*, 18242–18253. [CrossRef]
230. Wu, J.; Huang, C.; Liu, W.; Yin, A.; Chen, W.; He, C.; Wang, H.; Liu, S.; Fan, C.; Bowlin, G.L. Cell infiltration and vascularization in porous nanoyarn scaffolds prepared by dynamic liquid electrospinning. *J. Biomed. Nanotechnol.* **2014**, *10*, 603–614. [CrossRef]
231. Said, S.S.; Pickering, J.G.; Mequanint, K. Controlled delivery of fibroblast growth factor-9 from biodegradable poly (ester amide) fibers for building functional neovasculature. *Pharm. Res.* **2014**, *31*, 3335–3347. [CrossRef]
232. Said, S.S.; O'Neil, C.; Yin, H.; Nong, Z.; Pickering, J.G.; Mequanint, K. Concurrent and sustained delivery of FGF2 and FGF9 from electrospun poly (ester amide) fibrous mats for therapeutic angiogenesis. *Tissue Eng. Part A* **2016**, *22*, 584–596. [CrossRef] [PubMed]
233. Wong, H.K.; Lam, C.R.I.; Wen, F.; Chong, S.K.M.; Tan, N.S.; Jerry, C.; Pal, M.; Tan, L.P. Novel method to improve vascularization of tissue engineered constructs with biodegradable fibers. *Biofabrication* **2016**, *8*, 015004. [CrossRef] [PubMed]
234. He, S.; Xia, T.; Wang, H.; Wei, L.; Luo, X.; Li, X. Multiple release of polyplexes of plasmids VEGF and bFGF from electrospun fibrous scaffolds towards regeneration of mature blood vessels. *Acta Biomater.* **2012**, *8*, 2659–2669. [CrossRef] [PubMed]
235. Krishnan, L.; Touroo, J.; Reed, R.; Boland, E.; Hoying, J.B.; Williams, S.K. Vascularization and cellular isolation potential of a novel electrospun cell delivery vehicle. *J. Biomed. Mater. Res. Part A* **2014**, *102*, 2208–2219. [CrossRef] [PubMed]
236. Wang, Z.; Sun, B.; Zhang, M.; Ou, L.; Che, Y.; Zhang, J.; Kong, D. Functionalization of electrospun poly (ε-caprolactone) scaffold with heparin and vascular endothelial growth factors for potential application as vascular grafts. *J. Bioact. Compat. Polym.* **2013**, *28*, 154–166. [CrossRef]
237. Shafiq, M.; Jung, Y.; Kim, S.H. In situ vascular regeneration using substance P-immobilised poly (L-lactide-co-ε-caprolactone) scaffolds: Stem cell recruitment, angiogenesis, and tissue regeneration. *Eur. Cell Mater.* **2015**, *30*, 282–302. [CrossRef] [PubMed]
238. Chen, S.; Ge, L.; Wang, H.; Cheng, Y.; Gorantla, S.; Poluektova, L.Y.; Gombart, A.F.; Xie, J. Eluted 25-hydroxyvitamin D3 from radially aligned nanofiber scaffolds enhances cathelicidin production while reducing inflammatory response in human immune system-engrafted mice. *Acta Biomater.* **2019**, *97*, 187–199. [CrossRef]
239. Shan, Y.-H.; Peng, L.-H.; Liu, X.; Chen, X.; Xiong, J.; Gao, J.-Q. Silk fibroin/gelatin electrospun nanofibrous dressing functionalized with astragaloside IV induces healing and anti-scar effects on burn wound. *Int. J. Pharm.* **2015**, *479*, 291–301. [CrossRef]
240. Gao, J.; Wang, Y.; Chen, S.; Tang, D.; Jiang, L.; Kong, D.; Wang, S. Electrospun poly-ε-caprolactone scaffold modified with catalytic nitric oxide generation and heparin for small-diameter vascular graft. *RSC Adv.* **2017**, *7*, 18775–18784. [CrossRef]
241. Govindarajan, D.; Lakra, R.; Korapatti, P.S.; Ramasamy, J.; Kiran, M.S. Nanoscaled Biodegradable Metal–Polymeric Three-Dimensional Framework for Endothelial Cell Patterning and Sustained Angiogenesis. *ACS Biomater. Sci. Eng.* **2019**, *5*, 2519–2531. [CrossRef]
242. Kuttappan, S.; Mathew, D.; Jo, J.-i.; Tanaka, R.; Menon, D.; Ishimoto, T.; Nakano, T.; Nair, S.V.; Nair, M.B.; Tabata, Y. Dual release of growth factor from nanocomposite fibrous scaffold promotes vascularisation and bone regeneration in rat critical sized calvarial defect. *Acta Biomater.* **2018**, *78*, 36–47. [CrossRef] [PubMed]

243. Huang, Y.C.; Kaigler, D.; Rice, K.G.; Krebsbach, P.H.; Mooney, D.J. Combined angiogenic and osteogenic factor delivery enhances bone marrow stromal cell-driven bone regeneration. *J. Bone Miner. Res.* **2005**, *20*, 848–857. [CrossRef] [PubMed]
244. Lü, L.; Deegan, A.; Musa, F.; Xu, T.; Yang, Y. The effects of biomimetically conjugated VEGF on osteogenesis and angiogenesis of MSCs (human and rat) and HUVECs co-culture models. *Colloids Surfaces B Biointer.* **2018**, *167*, 550–559. [CrossRef]
245. Lee, J.-H.; Lee, Y.J.; Cho, H.-J.; Kim, D.W.; Shin, H. The incorporation of bFGF mediated by heparin into PCL/gelatin composite fiber meshes for guided bone regeneration. *Drug Deliv. Transl. Res.* **2015**, *5*, 146–159. [CrossRef] [PubMed]
246. Cheng, G.; Yin, C.; Tu, H.; Jiang, S.; Wang, Q.; Zhou, X.; Xing, X.; Xie, C.; Shi, X.; Du, Y. Controlled Co-delivery of Growth Factors through Layer-by-Layer Assembly of Core–Shell Nanofibers for Improving Bone Regeneration. *ACS Nano* **2019**, *13*, 6372–6382. [CrossRef]
247. Oliveira, H.; Catros, S.; Castano, O.; Rey, S.; Siadous, R.; Clift, D.; Marti-Munoz, J.; Batista, M.; Bareille, R.; Planell, J. The proangiogenic potential of a novel calcium releasing composite biomaterial: Orthotopic in vivo evaluation. *Acta Biomater.* **2017**, *54*, 377–385. [CrossRef]
248. Patel, J.J.; Modes, J.E.; Flanagan, C.L.; Krebsbach, P.H.; Edwards, S.P.; Hollister, S.J. Dual delivery of epo and bmp2 from a novel modular poly-ε-caprolactone construct to increase the bone formation in prefabricated bone flaps. *Tissue Eng. Part C Methods* **2015**, *21*, 889–897. [CrossRef] [PubMed]
249. Weng, L.; Boda, S.K.; Wang, H.; Teusink, M.J.; Shuler, F.D.; Xie, J. Novel 3D hybrid nanofiber aerogels coupled with BMP-2 peptides for cranial bone regeneration. *Adv. Healthc. Mater.* **2018**, *7*, 1701415. [CrossRef]
250. Ikeda, K.; Takeshita, S. Factors and mechanisms involved in the coupling from bone resorption to formation: How osteoclasts talk to osteoblasts. *J. Bone Metab.* **2014**, *21*, 163–167. [CrossRef]
251. Wang, Y.; Cui, W.; Zhao, X.; Wen, S.; Sun, Y.; Han, J.; Zhang, H. Bone remodeling-inspired dual delivery electrospun nanofibers for promoting bone regeneration. *Nanoscale* **2019**, *11*, 60–71. [CrossRef]
252. Bao, P.; Kodra, A.; Tomic-Canic, M.; Golinko, M.S.; Ehrlich, H.P.; Brem, H. The role of vascular endothelial growth factor in wound healing. *J. Surg. Res.* **2009**, *153*, 347–358. [CrossRef] [PubMed]
253. Tandara, A.A.; Mustoe, T.A. Oxygen in wound healing—More than a nutrient. *World J. Surg.* **2004**, *28*, 294–300. [CrossRef] [PubMed]
254. Tchemtchoua, V.T.; Atanasova, G.; Aqil, A.; Filée, P.; Garbacki, N.; Vanhooteghem, O.; Deroanne, C.; Noël, A.; Jérome, C.; Nusgens, B. Development of a chitosan nanofibrillar scaffold for skin repair and regeneration. *Biomacromolecules* **2011**, *12*, 3194–3204. [CrossRef] [PubMed]
255. Moura, L.I.; Dias, A.M.; Carvalho, E.; de Sousa, H.C. Recent advances on the development of wound dressings for diabetic foot ulcer treatment—A review. *Acta Biomater.* **2013**, *9*, 7093–7114. [CrossRef] [PubMed]
256. Chong, H.C.; Chan, J.S.K.; Goh, C.Q.; Gounko, N.V.; Luo, B.; Wang, X.; Foo, S.; Wong, M.T.C.; Choong, C.; Kersten, S. Angiopoietin-like 4 stimulates STAT3-mediated iNOS expression and enhances angiogenesis to accelerate wound healing in diabetic mice. *Mol. Ther.* **2014**, *22*, 1593–1604. [CrossRef] [PubMed]
257. Chen, H.; Guo, L.; Wicks, J.; Ling, C.; Zhao, X.; Yan, Y.; Qi, J.; Cui, W.; Deng, L. Quickly promoting angiogenesis by using a DFO-loaded photo-crosslinked gelatin hydrogel for diabetic skin regeneration. *J. Mater. Chem. B* **2016**, *4*, 3770–3781. [CrossRef]
258. Zhang, Q.; Oh, J.-H.; Park, C.H.; Baek, J.-H.; Ryoo, H.-M.; Woo, K.M. Effects of dimethyloxalylglycine-embedded poly (ε-caprolactone) fiber meshes on wound healing in diabetic rats. *ACS Appl. Mater. Interfaces* **2017**, *9*, 7950–7963. [CrossRef]
259. Senturk, B.; Mercan, S.; Delibasi, T.; Guler, M.O.; Tekinay, A.B. Angiogenic peptide nanofibers improve wound healing in STZ-induced diabetic rats. *ACS Biomater. Sci. Eng.* **2016**, *2*, 1180–1189. [CrossRef]
260. Ren, X.; Han, Y.; Wang, J.; Jiang, Y.; Yi, Z.; Xu, H.; Ke, Q. An aligned porous electrospun fibrous membrane with controlled drug delivery–an efficient strategy to accelerate diabetic wound healing with improved angiogenesis. *Acta Biomater.* **2018**, *70*, 140–153. [CrossRef]
261. Xie, Z.; Paras, C.B.; Weng, H.; Punnakitikashem, P.; Su, L.-C.; Vu, K.; Tang, L.; Yang, J.; Nguyen, K.T. Dual growth factor releasing multi-functional nanofibers for wound healing. *Acta Biomater.* **2013**, *9*, 9351–9359. [CrossRef]

262. Agarwal, A.; Nelson, T.B.; Kierski, P.R.; Schurr, M.J.; Murphy, C.J.; Czuprynski, C.J.; McAnulty, J.F.; Abbott, N.L. Polymeric multilayers that localize the release of chlorhexidine from biologic wound dressings. *Biomaterials* **2012**, *33*, 6783–6792. [CrossRef] [PubMed]
263. Su, X.; Kim, B.-S.; Kim, S.R.; Hammond, P.T.; Irvine, D.J. Layer-by-layer-assembled multilayer films for transcutaneous drug and vaccine delivery. *ACS Nano* **2009**, *3*, 3719–3729. [CrossRef]
264. Nguyen, T.T.T.; Ghosh, C.; Hwang, S.-G.; Chanunpanich, N.; Park, J.S. Porous core/sheath composite nanofibers fabricated by coaxial electrospinning as a potential mat for drug release system. *Int. J. Pharm.* **2012**, *439*, 296–306. [CrossRef] [PubMed]
265. Wang, X.; Lv, F.; Li, T.; Han, Y.; Yi, Z.; Liu, M.; Chang, J.; Wu, C. Electrospun micropatterned nanocomposites incorporated with Cu2S nanoflowers for skin tumor therapy and wound healing. *ACS Nano* **2017**, *11*, 11337–11349. [CrossRef]
266. Lundborg, G. *Nerve Injury and Repair: Regeneration, Reconstruction, and Cortical Remodeling*; Elsevier/Churchill Livingstone: Philadelphia, PA, USA, 2005.
267. Hu, J.; Zhu, Q.-T.; Liu, X.-L.; Xu, Y.-b.; Zhu, J.-K. Repair of extended peripheral nerve lesions in rhesus monkeys using acellular allogenic nerve grafts implanted with autologous mesenchymal stem cells. *Exp. Neurol.* **2007**, *204*, 658–666. [CrossRef] [PubMed]
268. Xu, C.; Inai, R.; Kotaki, M.; Ramakrishna, S. Aligned biodegradable nanofibrous structure: A potential scaffold for blood vessel engineering. *Biomaterials* **2004**, *25*, 877–886. [CrossRef]
269. Wang, H.B.; Mullins, M.E.; Cregg, J.M.; Hurtado, A.; Oudega, M.; Trombley, M.T.; Gilbert, R.J. Creation of highly aligned electrospun poly-L-lactic acid fibers for nerve regeneration applications. *J. Neural Eng.* **2008**, *6*, 016001. [CrossRef]
270. Schnell, E.; Klinkhammer, K.; Balzer, S.; Brook, G.; Klee, D.; Dalton, P.; Mey, J. Guidance of glial cell migration and axonal growth on electrospun nanofibers of poly-ε-caprolactone and a collagen/poly-ε-caprolactone blend. *Biomaterials* **2007**, *28*, 3012–3025. [CrossRef]
271. Chew, S.Y.; Mi, R.; Hoke, A.; Leong, K.W. Aligned protein–polymer composite fibers enhance nerve regeneration: A potential tissue-engineering platform. *Adv. Funct. Mater.* **2007**, *17*, 1288–1296. [CrossRef]
272. Liu, Q.; Huang, J.; Shao, H.; Song, L.; Zhang, Y. Dual-factor loaded functional silk fibroin scaffolds for peripheral nerve regeneration with the aid of neovascularization. *RSC Adv.* **2016**, *6*, 7683–7691. [CrossRef]
273. Colello, R.J.; Chow, W.N.; Bigbee, J.W.; Lin, C.; Dalton, D.; Brown, D.; Jha, B.S.; Mathern, B.E.; Lee, K.D.; Simpson, D.G. The incorporation of growth factor and chondroitinase ABC into an electrospun scaffold to promote axon regrowth following spinal cord injury. *J. Tissue Eng. Regen. Med.* **2016**, *10*, 656–668. [CrossRef] [PubMed]
274. Zhang, Y.; Huang, J.; Huang, L.; Liu, Q.; Shao, H.; Hu, X.; Song, L. Silk fibroin-based scaffolds with controlled delivery order of VEGF and BDNF for cavernous nerve regeneration. *ACS Biomater. Sci. Eng.* **2016**, *2*, 2018–2025. [CrossRef]
275. Xia, B.; Lv, Y. Dual-delivery of VEGF and NGF by emulsion electrospun nanofibrous scaffold for peripheral nerve regeneration. *Mater. Sci. Eng. C* **2018**, *82*, 253–264. [CrossRef] [PubMed]
276. Du, P.; Casavitri, C.; Suhaeri, M.; Wang, P.-Y.; Lee, J.H.; Koh, W.-G.; Park, K. A Fibrous Hybrid Patch Couples Cell-Derived Matrix and Poly (l-lactide-co-caprolactone) for Endothelial Cells Delivery and Skin Wound Repair. *ACS Biomater. Sci. Eng.* **2018**, *5*, 900–910. [CrossRef]
277. Zhang, Y.; Chang, M.; Bao, F.; Xing, M.; Wang, E.; Xu, Q.; Huan, Z.; Guo, F.; Chang, J. Multifunctional Zn doped hollow mesoporous silica/polycaprolactone electrospun membranes with enhanced hair follicle regeneration and antibacterial activity for wound healing. *Nanoscale* **2019**, *11*, 6315–6333. [CrossRef]
278. Wang, Y.; Chen, Z.; Luo, G.; He, W.; Xu, K.; Xu, R.; Lei, Q.; Tan, J.; Wu, J.; Xing, M. In-situ-generated vasoactive intestinal peptide loaded microspheres in mussel-inspired polycaprolactone nanosheets creating spatiotemporal releasing microenvironment to promote wound healing and angiogenesis. *ACS Appl. Mater. Interfaces* **2016**, *8*, 7411–7421. [CrossRef]
279. Samadian, H.; Salehi, M.; Farzamfar, S.; Vaez, A.; Ehterami, A.; Sahrapeyma, H.; Goodarzi, A.; Ghorbani, S. In vitro and in vivo evaluation of electrospun cellulose acetate/gelatin/hydroxyapatite nanocomposite mats for wound dressing applications. *Artif. Cell. Nanomed. Biotechnol.* **2018**, *46*, 964–974. [CrossRef]
280. Meka, S.R.K.; Kumar Verma, S.; Agarwal, V.; Chatterjee, K. In Situ Silication of Polymer Nanofibers to Engineer Multi-Biofunctional Composites. *ChemistrySelect* **2018**, *3*, 3762–3773. [CrossRef]

281. Jeon, J.-K.; Seo, H.; Park, J.; Son, S.J.; Kim, Y.R.; Kim, E.S.; Park, J.W.; Jung, W.-G.; Jeon, H.; Kim, Y.-C. Conceptual Study for Tissue-Regenerative Biodegradable Magnesium Implant Integrated with Nitric Oxide-Releasing Nanofibers. *Met. Mater. Int.* **2019**, *25*, 1098–1107. [CrossRef]
282. Yun, H.-M.; Kang, S.-K.; Singh, R.K.; Lee, J.-H.; Lee, H.-H.; Park, K.-R.; Yi, J.-K.; Lee, D.-W.; Kim, H.-W.; Kim, E.-C. Magnetic nanofiber scaffold-induced stimulation of odontogenesis and pro-angiogenesis of human dental pulp cells through Wnt/MAPK/NF-κB pathways. *Dent. Mater.* **2016**, *32*, 1301–1311. [CrossRef]

© 2020 by the authors. Licensee MDPI, Basel, Switzerland. This article is an open access article distributed under the terms and conditions of the Creative Commons Attribution (CC BY) license (http://creativecommons.org/licenses/by/4.0/).